Energy Reports 7 (2021) 136–157

Contents lists available at ScienceDirect

Energy Reports

journal homepage: www.elsevier.com/locate/egyr

Global solar radiation prediction over North Dakota using air temperature: Development of novel hybrid intelligence model

Hai Tao [a], Ahmed A. Ewees [b,c], Ali Omran Al-Sulttani [d], Ufuk Beyaztas [e], Mohammed Majeed Hameed [f], Sinan Q. Salih [g,h], Asaad M. Armanuos [i], Nadhir Al-Ansari [j], Cyril Voyant [k], Shamsuddin Shahid [l], Zaher Mundher Yaseen [m,*]

[a] School of Computer Science, Baoji University of Arts and Sciences, 721007, China
[b] Department of e-Systems, University of Bisha, Bisha 61922, Saudi Arabia
[c] Department of Computer, Damietta University, Damietta 34517, Egypt
[d] Department of Water Resources Engineering, College of Engineering, University of Baghdad, Baghdad, Iraq
[e] Department of Economics and Finance, Piri Reis University, Istanbul, Turkey
[f] Department of Civil Engineering, Al-Maaref University College, Ramadi, Iraq
[g] Institute of Research and Development, Duy Tan University, Da Nang 550000, Viet Nam
[h] Computer Science Department, Dijlah University College, Baghdad, Iraq
[i] Irrigation and Hydraulics Engineering Department, Civil Engineering Department, Faculty of Engineering, Tanta University, Egypt
[j] Civil, Environmental and Natural Resources Engineering, Lulea University of Technology, 97187, Lulea, Sweden
[k] University of Corsica, CNRS UMR SPE 6134, 20250 Corte, France
[l] School of Civil Engineering, Faculty of Engineering, Universiti Teknologi Malaysia (UTM), 81310, Johor Bahru, Malaysia
[m] Faculty of Civil Engineering, Ton Duc Thang University, Ho Chi Minh City, Viet Nam

ARTICLE INFO

Article history:
Received 10 July 2020
Received in revised form 14 September 2020
Accepted 7 November 2020
Available online 30 November 2020

Keywords:
Solar radiation
Metaheuristic algorithms
Optimizer
Renewable energy
North Dakota

ABSTRACT

Accurate solar radiation (SR) prediction is one of the essential prerequisites of harvesting solar energy. The current study proposed a novel intelligence model through hybridization of Adaptive Neuro-Fuzzy Inference System (ANFIS) with two metaheuristic optimization algorithms, Salp Swarm Algorithm (SSA) and Grasshopper Optimization Algorithm (GOA) (ANFIS-muSG) for global SR prediction at different locations of North Dakota, USA. The performance of the proposed ANFIS-muSG model was compared with classical ANFIS, ANFIS-GOA, ANFIS-SSA, ANFIS-Grey Wolf Optimizer (ANFIS-GWO), ANFIS-Particle Swarm Optimization (ANFIS-PSO), ANFIS-Genetic Algorithm (ANFIS-GA) and ANFIS-Dragonfly Algorithm (ANFIS-DA). Consistent maximum, mean and minimum air temperature data for nine years (2010–2018) were used to build the models. ANFIS-muSG showed 25.7%–54.8% higher performance accuracy in terms of root mean square error compared to other models at different locations of the study areas. The model developed in this study can be employed for SR prediction from temperature only. The results indicate the potential of hybridization of ANFIS with the metaheuristic optimization algorithms for improvement of prediction accuracy.

1. Introduction

Solar Radiation (SR) influences hydrological processes, agricultural production, ecological services, public health and atmospheric circulation and therefore, comprehensive knowledge of SR at any location is vital to understand its economic potential and environmental sustainability (Abedinia et al., 2019; Ben Othman et al., 2018; Ghimire et al., 2019). Moreover, SR is a decisive and critical parameter for solar energy generation and management (Charabi et al., 2016; Gao et al., 2019). The recent effort of the replacement of fossil fuel sources with renewable energy resources has made SR as an important meteorological variable to measure and simulate renewable energy potential of any location of interest (Bagal et al., 2018). At present, 24% of the total global energy supply comes from renewable energy sources (Awasthi et al., 2020). Solar energy shares only 8.7% of the total renewable energy supply. However, solar energy's share of overall renewable energy has risen exponentially from 0.04% in 2000 to 8.7% in 2018, reflecting an average annual growth rate of nearly 43% since 2000 (Naubi et al., 2016). The expansion of solar energy would continue, and it has been projected that global solar energy installation would expand by six folds by 2030 (Sharafati et al., 2019). Reliable estimation of SR including its annual and seasonal variability has paramount importance of estimating the

* Corresponding author.
E-mail address: yaseen@tdtu.edu.vn (Z.M. Yaseen).

https://doi.org/10.1016/j.egyr.2020.11.033

solar energy potential and capacity (Alipour et al., 2017; Hafezi et al., 2017).

Generally, a conversion process required for the use of solar energy when the site is equipped with a radiometric measurement station operating steadily for a long period. The required data can be obtained using various techniques like measuring SR data by cell references and pyranometers as well as satellite sensors (Hai et al., 2020; Hou et al., 2018). Nevertheless, in most regions of the world, these crucial measurements are not effortlessly accessible due to technical, institutional, and financial limitations (Badescu et al., 2013; Benmouiza and Cheknane, 2016). Additionally, some developing countries do not have the technical capabilities and skilled manpower required to manage monitoring equipment and maintenance operations (Beyaztas et al., 2019). Furthermore, an accurate estimation of SR for a longer period is not available in most of the regions of the world. Therefore, modeling SR to construct daily or hourly data has become an important field of research in recent years.

The integration processes of solar energy sources have gradually become the greatest obstacle for energy demand in recent decades. A principal source of global warming is the burning of fossil fuels such as oil and coal for energy generation in a conventional way. A rising number of countries around the world are paying considerable attention to environmental concerns like climate change, greenhouses, gas emissions, and global warming through the reduction of fossil fuel burning (AlOmar et al., 2020; Mathew et al., 2019; Tao et al., 2019; Xie et al., 2019). This significantly encouraged the utilization and exploitation of friendly and alternative sources of energy such as solar, wind power, and others (Jiang et al., 2015). Although the solar radiation is widely available, it has some properties that may hinder the efficiency and stability of power grid systems such as time-varying, intermittence, uncertainty and stochastic (Calif et al., 2013; Zeng et al., 2013). This presents a new challenging issue regarding the process of integrating the sources of solar energy into the power grids. Measuring all the properties of solar radiation requires relatively expensive sensors like radiometers, pyranometers, and pyrheliometers incorporated with data-acquisition software and hardware (Dong and Jiang, 2019). The installation of such equipment and sensors across the world are also time-consuming and cumbersome (Hussain and Alili, 2017). To address these obstacles, it is very necessary to develop reliable SR prediction models with easily available meteorological variables for accurate estimation of SR at any point of interest.

Modeling SR is much more challenging compared to any other meteorological variables (Bokde et al., 2020). The SR is scattered and absorbed by the atmosphere. Besides, several atmospheric and weather conditions like could cover, wind and rainfall influence the amount of SR reached to land surface (Budiyanto et al., 2020). On top of that, it is highly variable and random when estimated at the ground. Modeling such highly erratic and random variable using conventional statistical methods is always very difficult (Voyant et al., 2020). Several methodologies using conventional statistical approaches have been designed to predict SR using geographical and metrological data such as precipitation, sunshine, humidity, air temperature, longitude and latitude (Deo et al., 2016; Fan et al., 2018c,a; Feng et al., 2018; Gouda et al., 2018; Hassan et al., 2016; Loghmari et al., 2018; Okundamiya et al., 2016; Premalatha and Naveen, 2018; Zou et al., 2016). Most of the conventional methods showed poor performance in predicting SR (Mohanty et al., 2016). Besides, they are unstable and less reliable in case of missing values in the dataset. The performance of such methods is also found to deteriorate rapidly with time and therefore, unsuitable for long-term predictions.

Artificial intelligence (AI) models have been used in recent years for better prediction of SR, considering their ability to simulate complex and nonlinear relationships and ability to handle missing data (Benmouiza and Cheknane, 2016; Feng et al., 2020; Kisi et al., 2019; Ghimire et al., 2019; Hai et al., 2020; Quej et al. 2017; Üstün et al. 2020). Several AI models have been introduced for SR prediction including artificial neural network (ANN), regression tree, genetic programming, support vector regression, data mining, and fuzzy logic (FL) (Voyant et al., 2017). Among the AI models, Adaptive Neuro-Fuzzy Inference System (ANFIS), a combination of ANN and FL approaches is considered one of the most efficient modeling techniques (Yaseen et al., 2019). Several studies showed a higher efficiency of ANFIS in predicting SR. For example, classical and hybrid ANFIS model by integrating ANFIS with particle swarm optimization (PSO), genetic algorithm (GA) and differential evolution algorithm (DEA) were employed to predict monthly global SR from different metrological factors like maximum and minimum air temperature, rainfall, clearness index and sunshine duration at a station located in Kuala Terengganu, Malaysia (Halabi et al., 2018). The results showed that the hybrid ANFIS-PSA performs better in predicting SR than the other models. Classical models namely Multiple Linear Regression (MLR) and different types of AI models including ANFIS were developed for prediction of daily global SR in Iraq using different metrological parameters (Nourani et al., 2019). The results illustrated that ANFIS provides more accurate result compared to other predictive models. A comparative analysis of different AI models in SR prediction revealed ANFIS is the most suitable for SR simulation due to its ability to capture the uncertainty associated with time series data (Mohammadi et al., 2016). However, the major problem of this model is the tuning of ANFIS hyperparameters such as, the optimization of membership function parameters (Castillo and Melin, 2012). Therefore, the traditional ANFIS model was hybridized with different optimization algorithms in previous studies for improving its performance. Though the performance of the existing hybrid ANFIS model is encouraging, the prediction capability is still needed to be enhanced considering the importance of the accuracy needed in SR measurement. Besides, one of the major limitations of existing SR prediction models is the requirement of many variables as input which are not readily available in some regions due to the lack of monitoring network.

The feasibility metaheuristics algorithms have showed a remarkable progression in modeling several engineering problems (Katebi et al., 2019; Sadeghipour Chahnasir et al., 2018). A novel model by hybridizing ANFIS with two metaheuristics algorithms namely, Grasshopper Optimization Algorithm (GOA) and Salp Swarm Algorithm (SSA) is proposed in this study for the prediction of SR. Hybridization of AI model with SSA provides advantages of low computational cost and ease of implementation. However, the major drawbacks of this metaheuristic algorithms are low exploitation ability, slow convergence, and local optima entrapment. This study attempts to overcome these drawbacks of SSA by introducing a mutation approach using a novel metaheuristic, GOA with the SSA process which is referred to as muSG in this article. The muSG is used to train the ANFIS model to improve its prediction performance. The proposed approach is collectively called ANFIS-muSG in this article. The performance of the proposed ANFIS-muSG model was compared with ANFIS, ANFIS-GOA, ANFIS-SSA, ANFIS-Grey Wolf Optimizer (ANFIS-GWO), ANFIS-Particle Swarm Optimization (ANFIS-PSO), ANFIS-Genetic Algorithm (ANFIS-GA) and ANFIS-Dragonfly Algorithm (ANFIS-DA) to show its efficacy. It is expected that the novel model proposed in this study would able to address the challenge of low predictivity of existing SR models due to its high and irregular variability and randomness.

Table 1
The statistical characteristics of the investigated meteorological station over the North Dakota region, USA.

	Standard deviation	min	max	mean	skewness
Baker					
Maximum Temperature °F	26.03	−23.06	99.61	49.96	−0.317
Minimum Temperature °F	23.31	−31.47	71.38	29.98	−0.463
Mean Temperature °F	24.39	−27.27	85.49	39.97	−0.394
Total Solar Radiation MJ/m^2	198.05	16.59	756.30	330.35	0.353
Beach					
Maximum Temperature °F	24.02	−16.02	105.84	55.07	−0.322
Minimum Temperature °F	19.88	−32.62	70.45	31.59	−0.530
Mean Temperature °F	21.56	−22.35	84.23	43.33	−0.425
Total Solar Radiation MJ/m^2	196.50	28.08	761.76	342.44	0.323
Cando					
Maximum Temperature °F	26.22	−17.79	101.70	50.00	−0.299
Minimum Temperature °F	23.88	−32.24	71.74	28.32	−0.481
Mean Temperature °F	24.70	−24.99	83.86	39.16	−0.394
Total Solar Radiation MJ/m^2	193.75	14.21	754.27	321.56	0.365
Crary					
Maximum Temperature °F	25.87	−18.96	101.37	50.21	−0.306
Minimum Temperature °F	23.45	−28.01	73.22	30.88	−0.446
Mean Temperature °F	24.39	−23.49	82.90	40.54	−0.378
Total Solar Radiation	194.03	15.50	729.86	320.89	0.377
Fingal					
Maximum Temperature °F	25.55	−17.25	97.11	52.05	−0.333
Minimum Temperature °F	22.87	−27.51	72.97	32.21	−0.432
Mean Temperature °F	23.94	−21.51	83.80	42.13	−0.385
Total Solar Radiation MJ/m^2	191.47	0.00	739.21	326.51	0.321

2. Case study and data explanation

Being located in the middle of North America, the climate of North Dakota (ND) is characterized by cold winters and hot summers, coupled with large variations in temperature which results in varying weather conditions. The climate conditions also vary in the eastern and western parts of ND. The Köppen–Geiger climate classification system categorized the eastern part of ND as a humid continental climate while the western part as semi-arid climate (Peel et al., 2007). Table 1 reports the statistical characteristics of maximum, minimum, mean, standard deviation and skewness of air temperature and total solar radiation estimated at five meteorological stations namely, Baker, Beach, Cando, Crary, and Fingal in ND (Fig. 1) for the period 2010–2018. The data were divided into 70%–30% for training and testing the developed and benchmark models. The dataset were obtained from an open source website (https://ndawn.ndsu.nodak.edu). Based on the reported statistical measures of the utilized dataset, a slight variation in temperature and SR were observed among all the inspected stations. The maximum temperature of 105.84 °F was recoded at Beach station while the maximum total SR was estimated as 756.30 MJ/m^2 at Baker station.

3. Methodological overview

3.1. Adaptive Neuro-Fuzzy Inference System (ANFIS)

ANFIS, a combination of FL and ANN is developed by Jang and Sun (1995) to take the advantages of FL and ANN. A typical ANFIS model has five layers as illustrated in Fig. 2.

The first layer transfers its inputs to the nodes to compute its output using generalized Gaussian membership (GGM) function as follows (Sedghi et al., 2018):

$$O_{1i} = \mu_{A_i}(x), \; i = 1, 2, \qquad (1)$$
$$O_{1i} = \mu_{B_{i-2}}(y), \; i = 3, 4$$
$$\mu(x) = e^{-(x-\rho_i/\sigma_i)^2} \qquad (2)$$

where B_i and A_i are the membership values, μ is the GGM, σ_i and ρ_i are the premise variable set.

The second layer computes the result of each node and the third layer normalizes the results using Eqs. (3) and (4), respectively,

$$O_{2i} = \omega_i = \mu_{A_i}(x) \times \mu_{B_{i-2}}(y) \qquad (3)$$
$$O_{3i} = \overline{w}_i = \frac{\omega_i}{\sum_{i=1}^{2} \omega_i}, \qquad (4)$$

The fourth layer computes the adaptive nodes using the following formula,

$$O_{4,i} = \overline{w}_i f_i = \overline{w}_i (p_i x + q_i y + r_i) \qquad (5)$$

where r, q, and p define the consequent variables of the ith node.

The fifth layer uses Eq. (6) to calculate the output.

$$O_5 = \sum_{i}^{\overline{w}_i} f_i \qquad (6)$$

In general, the search space in ANFIS during data processing may become wider and slower which can cause trapping to local minima. The optimization of ANFIS parameters can help to solve this issue.

3.2. Salp Swarm Algorithm (SSA)

SSA is an optimization technique proposed by Mirjalili et al. (2017) which mimics the real salp chains that a swarm uses for foraging and moving to reach a food source (Sutherland, 2017). This conduct is converted to a mathematical form for the development of SSA technique. In SSA, the population is split into two groups, leader and followers. The leader is found in front of the followers. To update the position of a group, the leader changes his position which can be expressed as:

$$x_j^i = \begin{cases} F_j + c_1((ub_j - lb_j) \times c_2 + lb_j), & c_3 \le 0 \\ F_j - c_1((ub_j - lb_j) \times c_2 + lb_j), & c_3 > 0 \end{cases} \qquad (7)$$

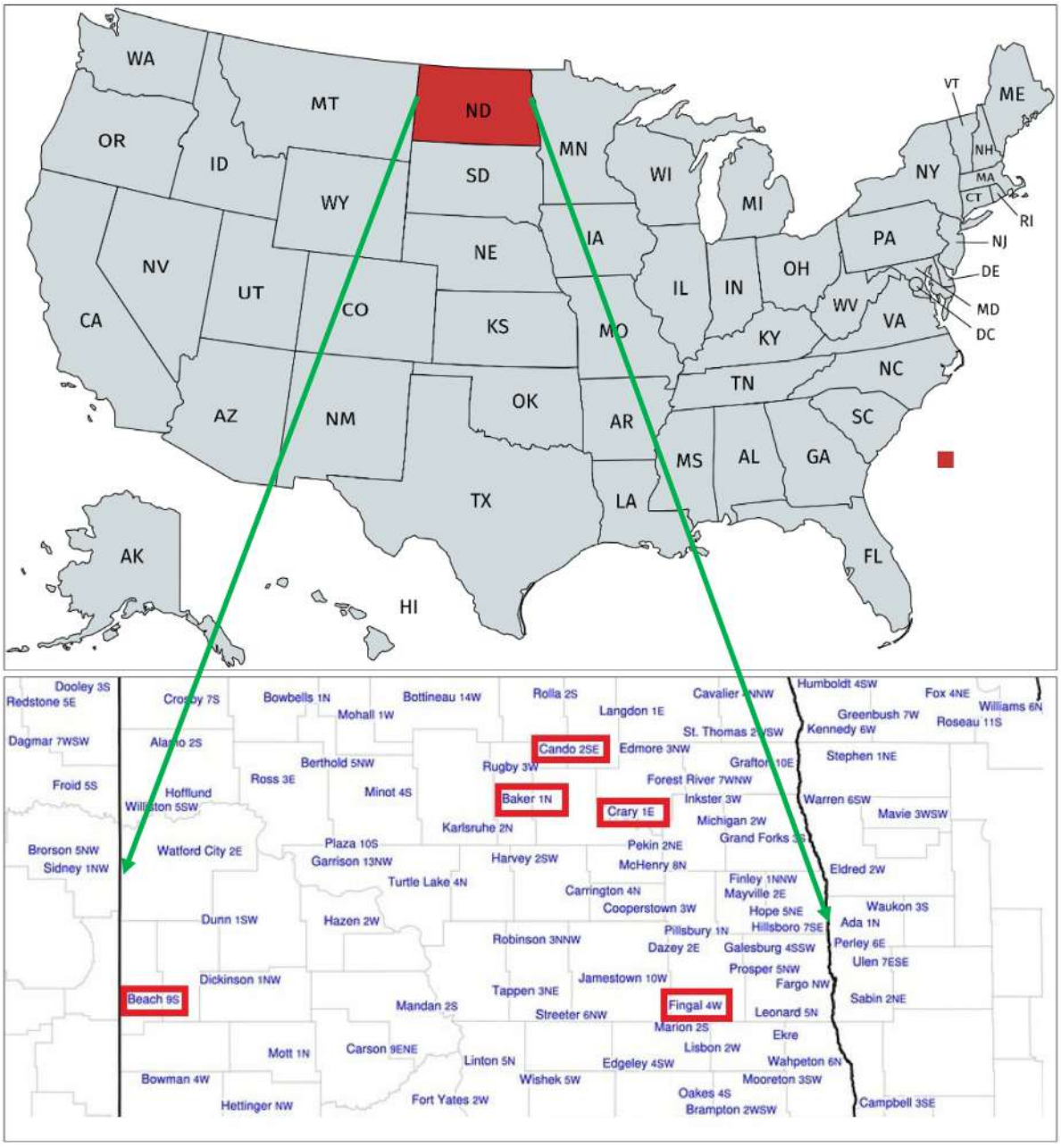

Fig. 1. The locations of the meteorological stations of North Dakota, USA used in this study.

where x_j^1 defines the position, ub_j and lb_j represent the upper and lower boundaries of the search domain jth, the target is defined by F_j, c_2 and c_3 define random parameters [0, 1] where the value of c_1 is computed as:

$$c_1 = 2e^{-\left(\frac{4t}{t_{max}}\right)^2} \tag{8}$$

where, t_{max} defines the max loop number and the current loop is defined by t.

The position of the followers is updated based on Eq. (9).

$$x_j^i = \frac{1}{2}(x_j^i + x_j^{i-1}) \tag{9}$$

where $i > 1$ and x_j^i denotes the ith follower position.

3.3. Grasshopper Optimization Algorithm (GOA)

GOA is an optimization technique developed by Saremi et al. (2017) to emulate the nature of grasshopper insects. In the early stage, the grasshopper cannot fly a long distance. Therefore, it employs a swarm behavior to travel a long distance. This behavior can mathematically be represented as:

$$x_i = S_i + G_i + A_i, \quad i = 1, 2, \ldots, N \tag{10}$$

where x_i represents the grasshopper position in i-th dimension. S_i represents the social interaction which can be expressed as:

$$S_i = \sum_{\substack{j=1 \\ i \neq j}}^{N} s(d_{ij})\hat{d}_{ij}, \qquad d_{ij} = \left|x_i - x_j\right|, \qquad \hat{d}_{ij} = \frac{x_i - x_j}{d_{ij}} \tag{11}$$

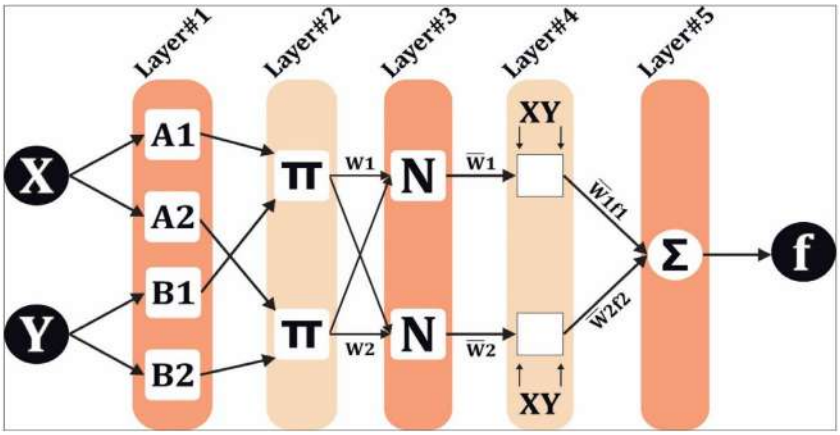

Fig. 2. The structure of adaptive neuro-fuzzy inference system model layers.

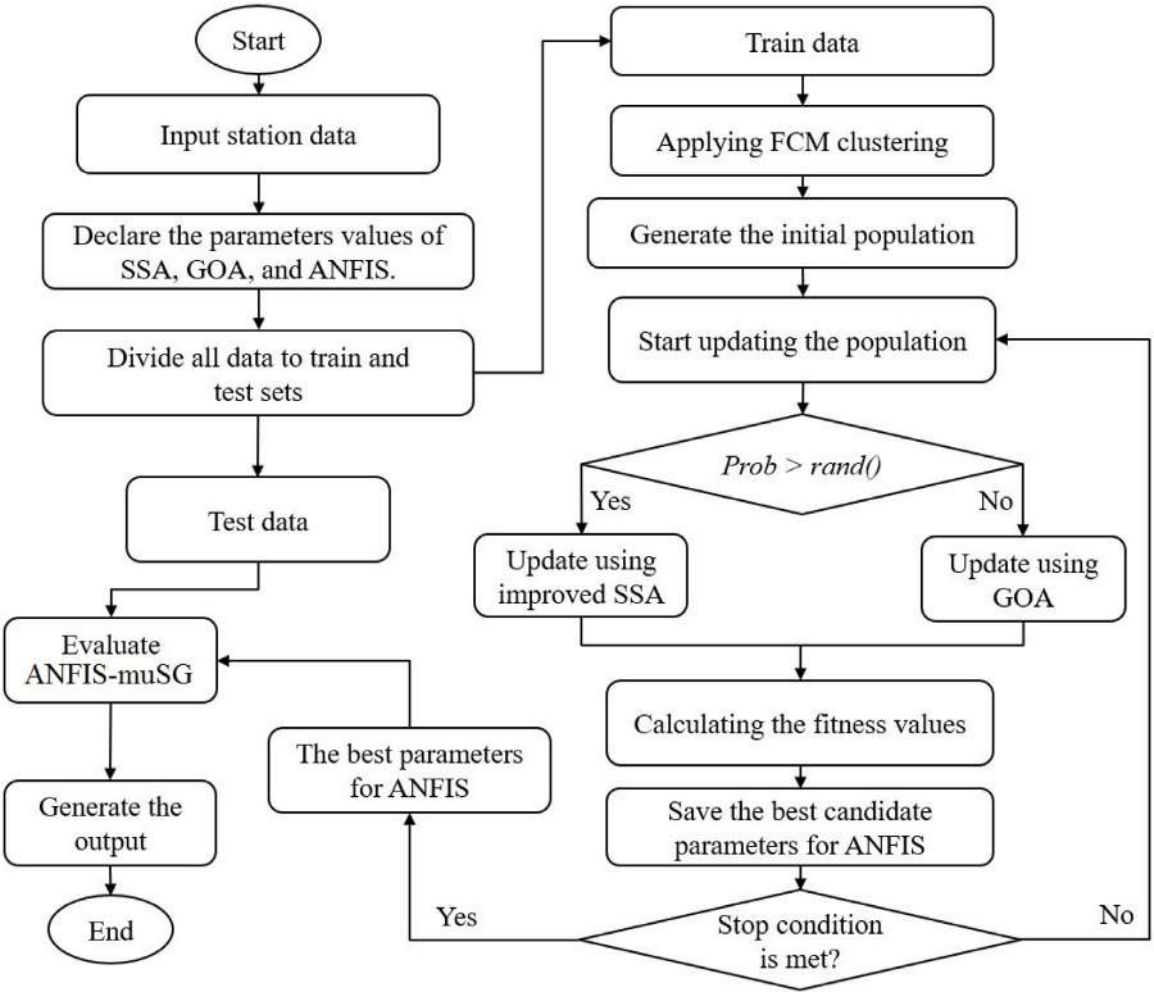

Fig. 3. The phases of the proposed methodology ANFIS-muSG.

where d_{ij} and $\hat{d}_{ij}$ represent the distance and a unit vector between grasshoppers, respectively. The parameter s can be defined as:

$$s(y) = fe^{\frac{-y}{l}} - e^{-y} \tag{12}$$

here, l and f represent the scale of the attractive length and the intensity of the attraction, respectively.

Besides, the small grasshoppers' movements are affected by the wind and gravity which can be expressed as,

$$\text{Wind advection} = A_i = u\hat{e}_w, \quad \text{Gravity force} = G_i = -g\hat{e}_g \tag{13}$$

here, u and $\hat{e}_w$ represent a constant drift and the wind direction unit vector, respectively, g and $\hat{e}_g$ represent the gravitational constant and the unity vector towards earth's center, respectively.

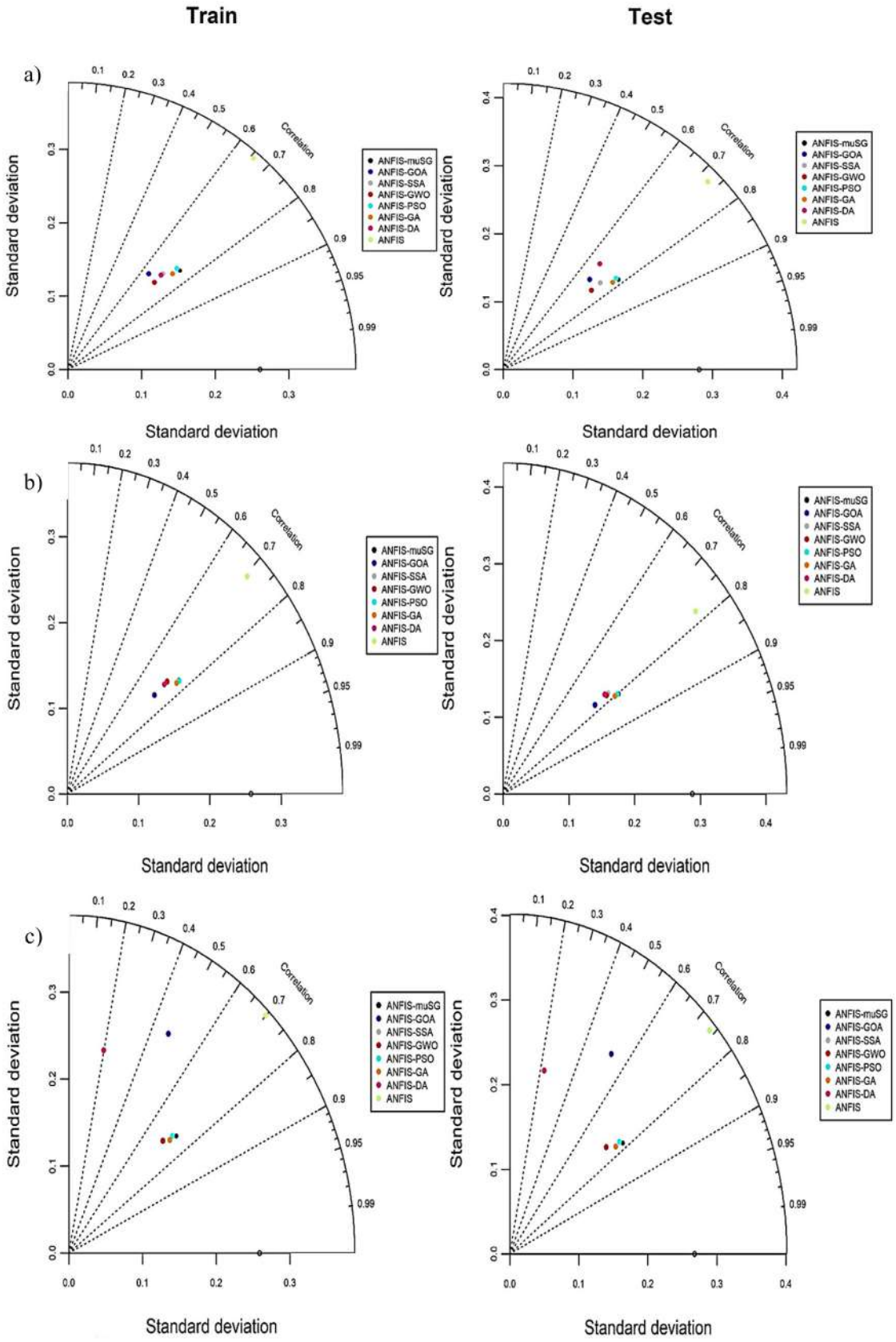

Fig. 4. Taylor diagram showing the performance of the solar radiation prediction models during training and testing phases at (a) Baker, (b) Beach, (c) Cando, (d) Crary, and (e) Fingal station.

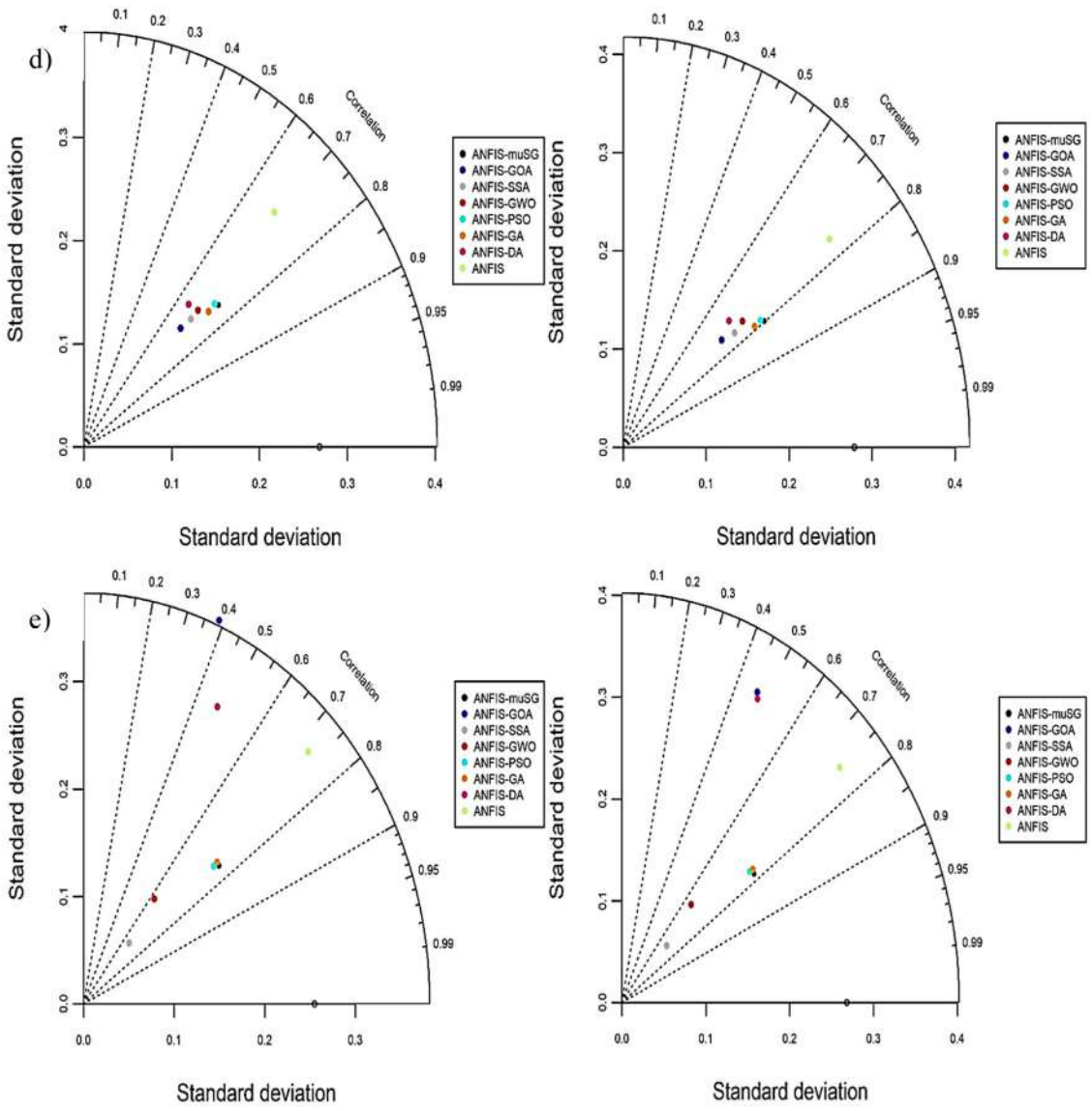

Fig. 4. (*continued*).

Consequently, the position of the grasshoppers is updated using the following equation.

$$x_i^d = c\left(\sum_{\substack{j=1\\ i\neq j}}^{N} c\frac{u_d - l_d}{2} s(|x_j^d - x_i^d|)\frac{x_j - x_i}{d_{ij}}\right) + \hat{T}_d, \tag{14}$$

where u and l represent the upper and lower boundaries of the searching space, respectively, and $\hat{T}_d$ is the value of the best solution. The problem dimension and the population size are represented by D and N, respectively and the parameter c is computed as,

$$c = c_{max} - t\frac{c_{max} - c_{min}}{t_{max}} \tag{15}$$

where c_{max} and c_{min} equal to 1 and 0.0001, respectively, t_{max} defines the max loop number whereas, the current loop is defined by t.

3.4. The proposed ANFIS-muSG model

The proposed ANFIS-muSG (ANFIS mutation salp swarm algorithm and grasshopper optimization algorithm) includes two phases. The first phase, called muSG, applies the mutation technique to improve the steps of SSA algorithm and uses the enhanced SSA as a local search to improve the GOA exploration ability. The second phase uses muSG for training the parameters of the original ANFIS model. Fig. 3 illustrates the phases of the proposed method. The descriptions of the phases are elaborated below.

i. **First phase**

In the first phase, a mutation technique is used to update the structure of the original SSA. A mutate vector x_{mu} is created as follows:

$$x_{mu,i} = x_q + \delta \times (x_w - x_r) \tag{16}$$

where, $i = 1, 2, 3, \ldots, N$; x_q, x_w, and x_r are randomly selected from the populations; and δ is in the range $[0, 2]$.

Then a new solution vector ($x_{mu,i}$) is tested using the objective function to determine its usability. The new structure of the SSA algorithm works as a local search for the original GOA algorithm.

ii. **Second phase:**

In this phase, the improved muSG is applied to train the ANFIS model to determine the weights and biases parameters

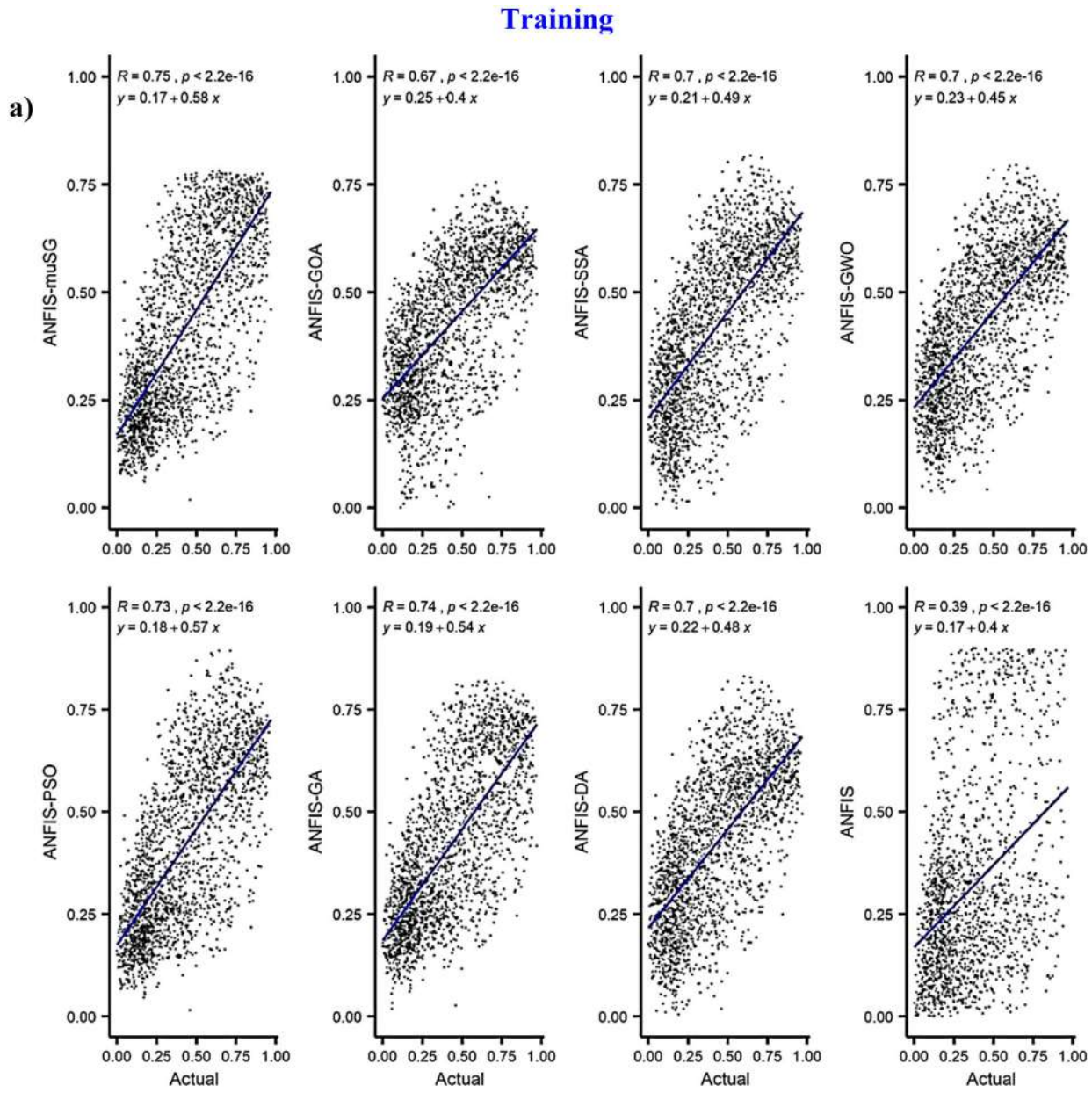

Fig. 5. The scatterplots showing the performance of the solar radiation predictive model during training and testing phases at (a) Baker, (b) Beach, (c) Cando, (d) Crary and (e) Fingal.

between the fourth and fifth layers because these parameters are chosen randomly. This optimization can lead to speed up time-to-convergence considerably and reduce the training error to produce a better prediction.

The steps of the proposed ANFIS-muSG begin by determining all parameter values and receiving the input values of the given problem. Then it splits the input to training and testing sets and applies fuzzy c-mean method as a membership function (Kisi and Yaseen, 2019). The muSG works to adapt the weights of ANFIS model by searching the optimal parameters to provide the best solution of a given problem. The obtained parameters are passed to improve the ANFIS model. The quality of the obtained parameters is evaluated using a fitness function:

$$MSE = \frac{1}{n}\sum_{i=1}^{n}(a_i - p_i)^2 \quad (17)$$

where, the actual and predicted values are defined by a and p, respectively, and n represents the input length.

The proposed method is repeated until it reaches the stop condition which is set in this study to the maximum number of iterations as proposed by Mirjalili et al. (2017). After finishing the training phase, the optimal parameters are used to solve the given problem with testing data.

3.5. Model development

The main goal of this study is to evaluate the efficacy of the proposed ANFIS-muSG approach in the prediction of daily SR. The model was developed using MATLAB 2014b software in a computer with an Intel Core i5 and 4 GB of RAM. The training phase of ANFIS-muSG starts by producing a population x randomly; where each x_i contains one solution (i = 1, 2, …., N). The solutions are updated using both GOA and the improved SSA based on a

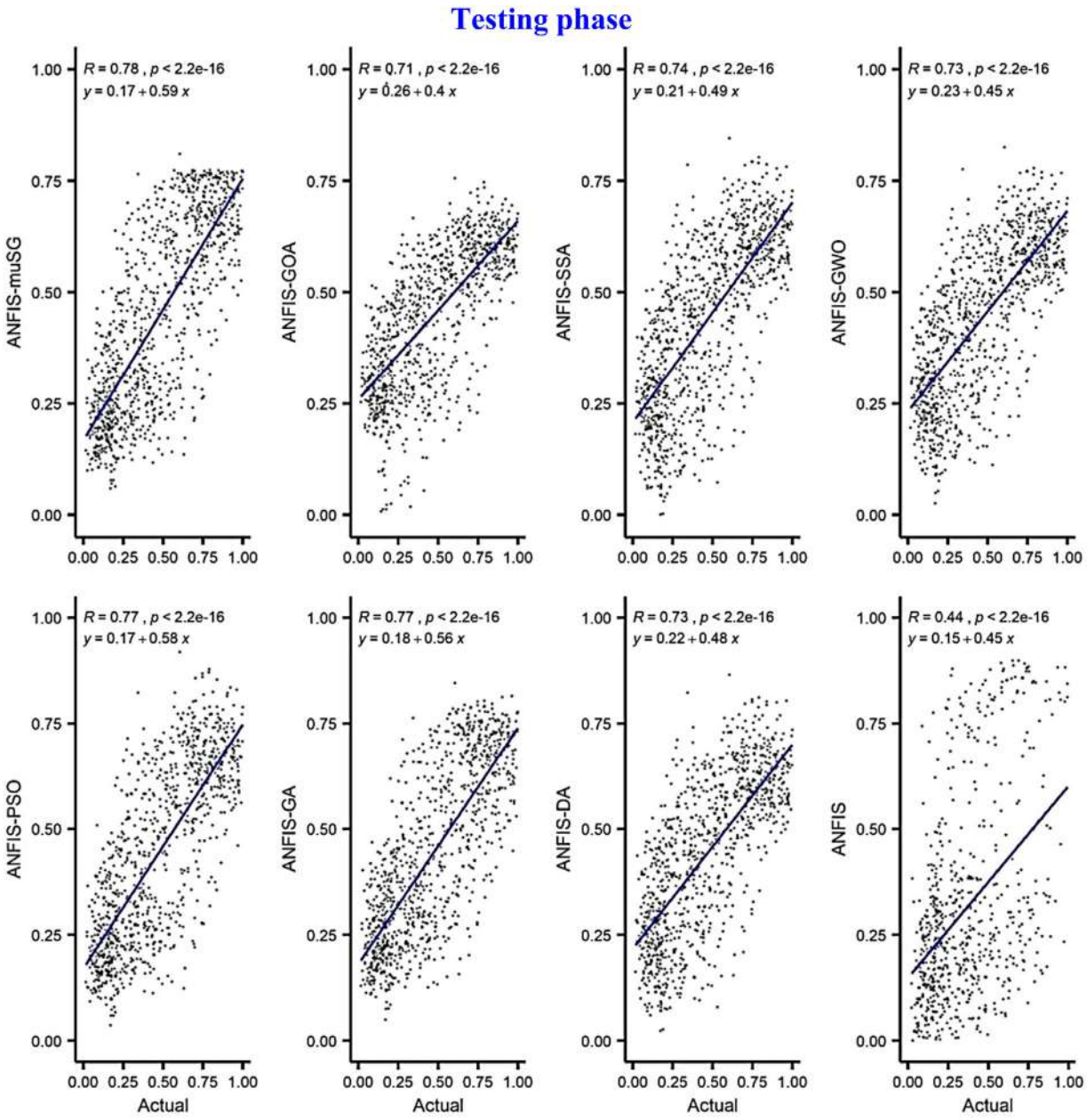

Fig. 5. (*continued*).

probability (pl) which is defined as,

$$pl_i = \frac{f_i}{\sum_{i=1}^{n} f_i} \tag{18}$$

where, f_i is the current fitness value (which can be calculated using Eq. (7)). If pl_i < *rand*(), the GOA algorithm is used, else the improved SSA is applied. The muSG helps GOA to overcome the drawbacks of the classic version of GOA, for instance, the premature convergence, getting trap in a local minimum, and the high computation time. The current solution is tested using fitness function (Eq. (17)) to determine the quality of the current solution. These steps are iterated until the maximum iteration limit is reached. The best parameters are used to improve the original ANFIS model be to applied on test data. The performance of the model for the testing data is evaluated using a set of measures as shown in Section 3.6. It is worth to mention, data were normalized into a scale between (0–1) and used for modeling SR in the present study to remove the influence of individual variables.

3.6. Performance metrics

Six statistical metrics namely, root mean square error (RMSE), mean absolute error (MAE), mean absolute relative error (MARE) root mean squared relative error (RMSRE), average absolute percent relative error (AAPRE) and coefficient of determination (R^2) were used to assess model performance. The formulas used to estimate the metrics are given below (AlOmar et al., 2020; Zhang et al., 2020):

$$RMSE = \sqrt{\frac{1}{n}\sum_{i=1}^{n}(a_i - p_i)^2} \tag{19}$$

$$MAE = \frac{1}{n}\sum_{i=1}^{n}|a_i - p_i| \tag{20}$$

$$MARE = \frac{1}{n}\sum_{i=1}^{n}\left(\left|\frac{a_i - p_i}{a_i}\right|\right) \tag{21}$$

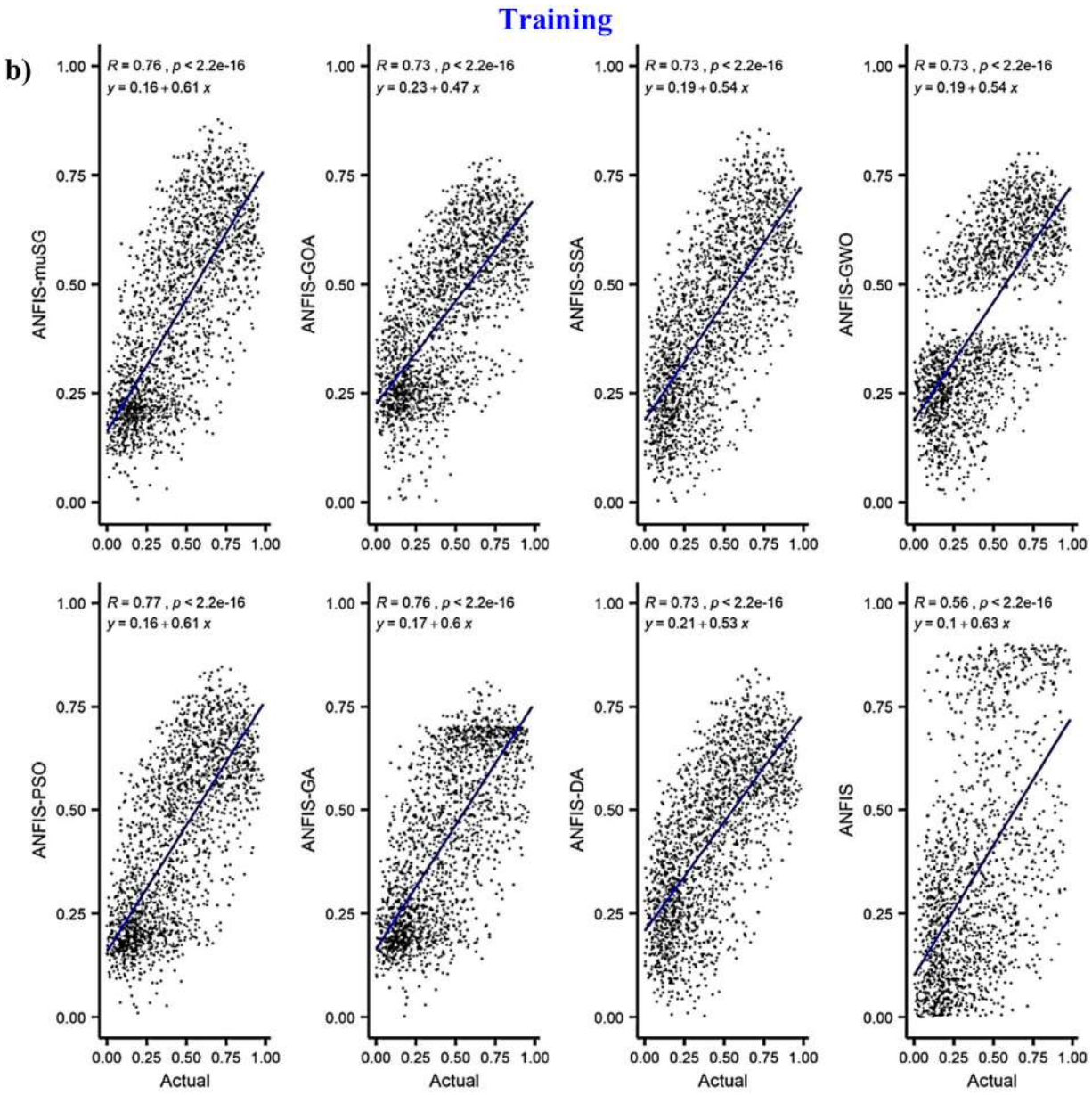

Fig. 5. (*continued*).

$$RMSRE = \sqrt{\frac{1}{n}\sum_{i=1}^{n}\left(\frac{a_i - p_i}{a_i}\right)^2} \tag{22}$$

$$AAPRE = \frac{100}{n}\sum_{i=1}^{n}\left(\left|\frac{a_i - p_i}{p_i}\right|\right) \tag{23}$$

$$R^2 = 1 - \frac{\sum(a_i - p_i)^2}{\sum(a_i - \mu_a)^2} \tag{24}$$

where, where a denotes the output values and p denotes the real values. n is the total number of items, and μ_a is the mean of a.

4. Application results and analysis

Statistical performance metrics and graphical visualization were used to assess the prediction capacity of the models. The performance of the models based on statistical metrics at Baker, Beach, Cando, Crary, and Fingal are provided in Tables 2 to 6, respectively. All the statistical metrics indicate better performance of the proposed ANFIS-muSG model compared to other models in the prediction of SR at all the stations. At Baker station, the ANFIS-muSG model showed lower values of error metrics (RMSE $\approx$ 0.179, MAE $\approx$ 0.145, MRE ≈ -30.213, MARE $\approx$ 0.568, RMSRE $\approx$ 1.254, and AAPRE $\approx$ 56.764). Similar lower error metrics were observed at other stations such as Beach (RMSE $\approx$ 0.174, MAE $\approx$ 0.140, MRE ≈ -34.183, MARE $\approx$ 0.611, RMSRE $\approx$ 3.010, and AAPRE $\approx$ 61.106), Cando (RMSE $\approx$ 0.168, MAE $\approx$ 0.136, MRE ≈ -34.639, MARE $\approx$ 0.583, RMSRE $\approx$ 1.232, and AAPRE $\approx$ 58.286), Crary (RMSE $\approx$ 0.170, MAE $\approx$ 0.137, MRE ≈ -42.22, MARE $\approx$ 0.653, RMSRE $\approx$ 4.087, and AAPRE $\approx$ 65.26) and Fingal (RMSE $\approx$ 0.171, MAE $\approx$ 0.136, MRE ≈ -29.181, MARE $\approx$ 0.516, RMSRE $\approx$ 0.976, and AAPRE $\approx$ 51.516).

The superiority of the ANFIS-muSG model was measured based on its capacity for reduction of RMSE during the testing phase. The results revealed a prediction enhancement by 42.2% using the ANFIS-muSG model compared to the stand-alone ANFIS model. ANFIS-PSO and ANFIS-GA also showed a very similar prediction performance though ANFIS-muSG was always found to perform a bit superior compared to them. The improvement in RMSE

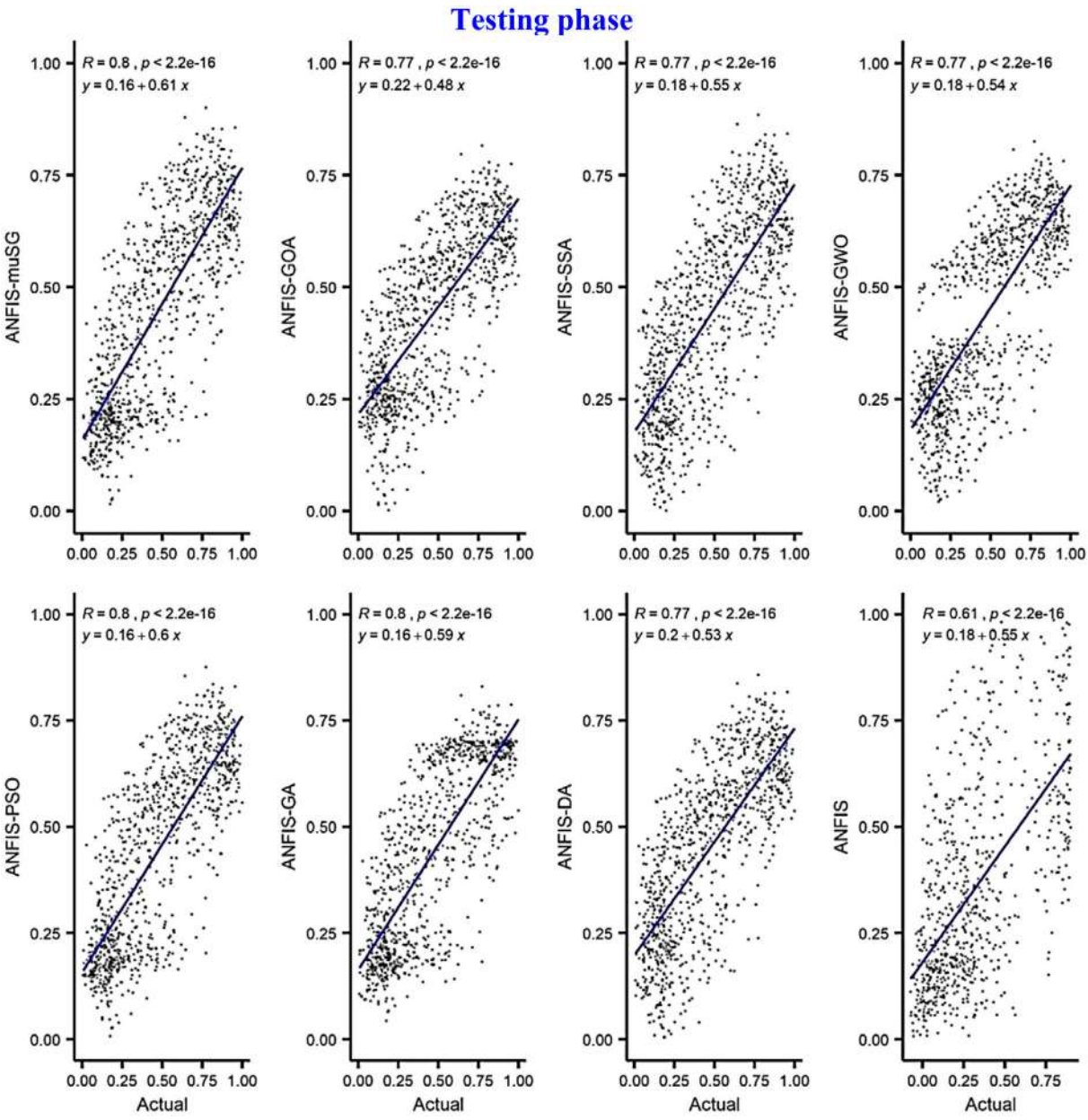

Fig. 5. (*continued*).

Table 2
The statistical performance of solar radiation prediction models during the testing phase at Baker station (bold represents the best result).

	RMSE MJ/m^2	MAE MJ/m^2	MRE	MARE	RMSRE	AAPRE	R^2	Time
ANFIS-mSG	**0.179**	**0.145**	−30.213	**0.568**	**1.254**	**56.764**	**0.774**	30.486
ANFIS-GOA	0.268	0.212	**−24.707**	0.904	3.506	90.406	0.596	39.312
ANFIS-SSA	0.193	0.160	−38.004	0.674	1.894	67.448	0.735	7.276
ANFIS-GWO	0.194	0.161	−41.536	0.693	2.051	69.276	0.736	7.849
ANFIS-PSO	0.181	0.146	−29.796	0.573	1.269	57.316	0.770	6.632
ANFIS-GA	0.180	0.146	−33.155	0.592	1.409	59.222	0.770	7.411
ANFIS-DA	0.232	0.181	−33.869	0.771	2.961	77.148	0.645	11.845
ANFIS	0.310	0.258	−87.668	1.072	4.698	107.187	0.702	**2.965**

by the proposed model at different locations are reported in Table 2. At Beach station, the ANFIS-muSG model showed a prediction augmentation by 32.6% compared to the ANFIS model. The prediction improvement at Cando, Crary, and Fingal stations were found 54.8, 25.7, and 49.0%, respectively. Among all the ANFIS models, the ANFIS-muSG model provided the height values for correlation coefficient ($R^2 \approx 0.77$, 0.80, 0.77, 0.79 and 0.76 at Baker, Beach, Cando, Crary and Fingal stations, respectively). The obtained results confirmed that the proposed ANFIS-muSG model can provide a more accurate and reliable prediction of SR in the study areas.

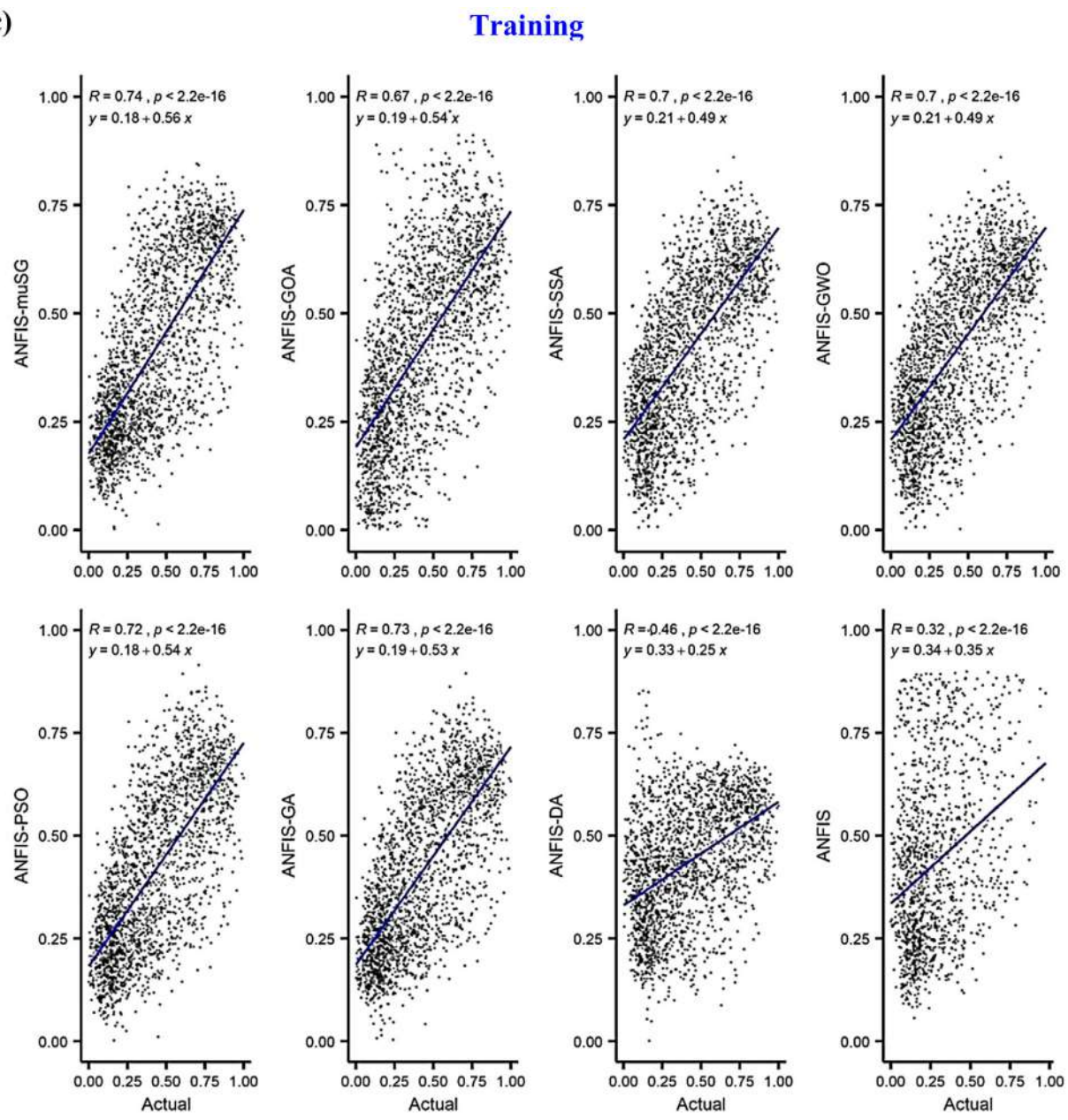

Fig. 5. (*continued*).

Table 3
The statistical performance of solar radiation prediction models during the testing phase at Beach station (bold represents the best result).

	RMSE MJ/m^2	MAE MJ/m^2	MRE	MARE	RMSRE	AAPRE	R^2	Time
ANFIS-mSG	**0.1744**	**0.1403**	−34.183	**0.611**	**3.010**	**61.106**	**0.802**	37.412
ANFIS-GOA	0.1897	0.1562	−45.782	0.761	4.726	76.056	0.766	40.786
ANFIS-SSA	0.1862	0.1523	−40.333	0.708	3.848	70.755	0.773	7.501
ANFIS-GWO	0.1863	0.1522	−42.005	0.716	4.107	71.567	0.774	7.981
ANFIS-PSO	0.1746	0.1404	**−33.913**	0.614	3.022	61.418	0.801	6.621
ANFIS-GA	0.1757	0.1413	−34.982	0.623	3.102	62.284	0.798	7.598
ANFIS-DA	0.1865	0.1526	−43.181	0.725	4.241	72.459	0.773	11.393
ANFIS	0.2588	0.2127	−12.884	0.785	3.579	78.489	0.773	**3.56**

The convergence time of the predictive models at different stations is also presented in Tables 2–6. The results showed that ANFIS-muSG model took more time for learning compared to other models, except ANFIS-GOA. High computational time is normal for such a metaheuristic optimization process (Ghadimi et al., 2018). However, the main advantage of such models is to increase the prediction accuracy of SR.

The performance of the models in simulation of the observed SR at all the five locations is visually presented using Taylor diagram in Fig. 4. Taylor diagram provides a measure of association,

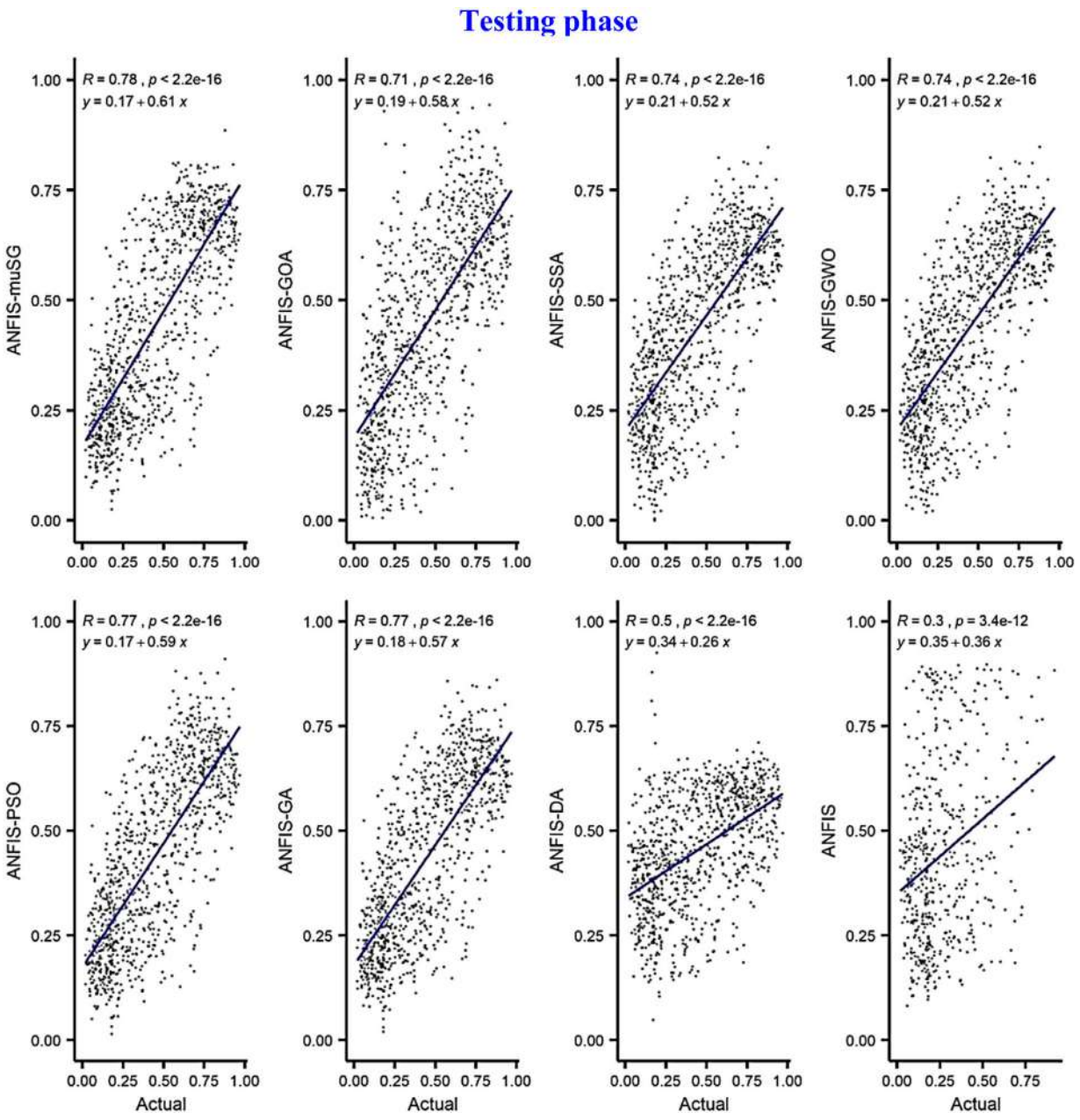

Fig. 5. (*continued*).

Table 4
The statistical performance of solar radiation prediction models during the testing phase at Cando station (bold represents the best result).

	RMSE MJ/m^2	MAE MJ/m^2	MRE	MARE	RMSRE	AAPRE	R^2	Time
ANFIS-mSG	**0.1687**	**0.1367**	−34.639	**0.583**	**1.232**	**58.286**	**0.777**	29.367
ANFIS-GOA	0.2863	0.2120	−58.813	1.044	5.792	104.398	0.565	39.061
ANFIS-SSA	0.1808	0.1499	−41.864	0.681	1.785	68.093	0.740	7.256
ANFIS-GWO	0.1800	0.1491	−42.373	0.677	1.774	67.742	0.743	7.858
ANFIS-PSO	0.1710	0.1390	**−34.269**	0.586	1.261	58.613	0.769	6.520
ANFIS-GA	0.1705	0.1386	−34.265	0.588	1.278	58.844	0.772	7.400
ANFIS-DA	0.2953	0.2318	−67.559	1.151	8.767	115.126	0.617	11.217
ANFIS	0.3733	0.3093	−70.127	1.068	3.553	106.846	0.725	**2.915**

variability, and error in simulated SR compared to the observed SR and thus, gives a detailed appraisal of model performance. Fig. 4 clearly showed that the ANFIS-muSG simulated SR closer to the observed SR as compared to other models during both training and testing phases. The results indicated significantly higher prediction accuracy of ANFIS-muSG model compared to other ANFIS models.

Fig. 5 presents the scatterplots of predicted and observed SR during model training and testing phases at all the studied stations. The scatterplots provide a more informative visualization of

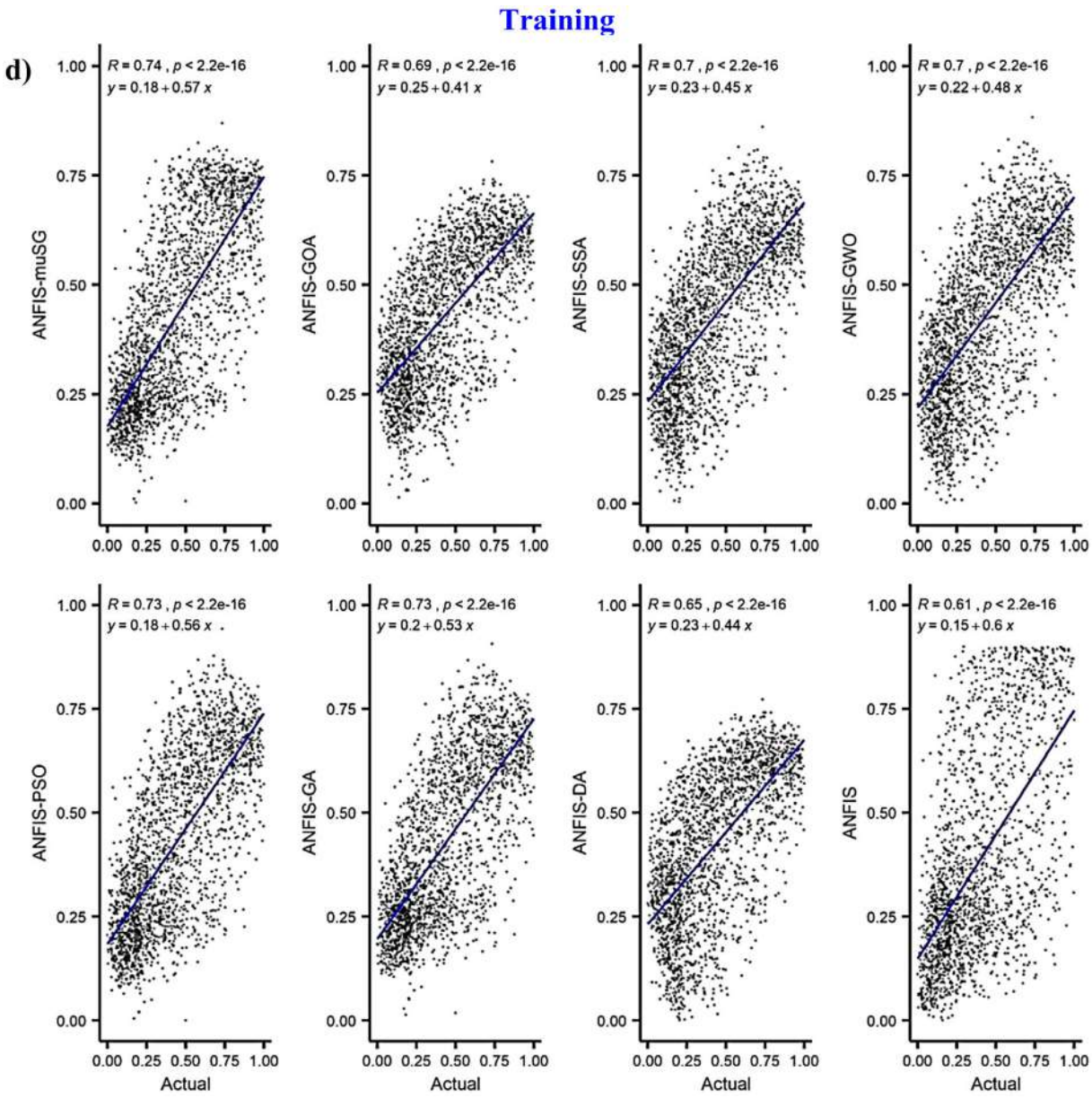

Fig. 5. (*continued*).

Table 5
The statistical performance of solar radiation prediction models during the testing phase at Crary station (bold represents the best result).

	RMSE MJ/m^2	MAE MJ/m^2	MRE	MARE	RMSRE	AAPRE	R^2	Time
ANFIS-mSG	**0.170**	**0.137**	−42.225	**0.653**	**4.087**	**65.263**	**0.794**	30.984
ANFIS-GOA	0.199	0.163	−56.855	0.877	11.948	87.713	0.710	40.279
ANFIS-SSA	0.187	0.155	−55.444	0.829	9.116	82.943	0.749	7.208
ANFIS-GWO	0.191	0.159	−60.160	0.855	10.793	85.514	0.732	8.088
ANFIS-PSO	0.172	0.139	**−41.859**	0.659	4.140	65.924	0.788	6.609
ANFIS-GA	0.172	0.139	−42.897	0.666	4.362	66.564	0.789	7.470
ANFIS-DA	0.198	0.162	−60.700	0.877	12.286	87.745	0.711	11.839
ANFIS	0.229	0.183	−44.980	0.730	4.472	72.982	0.704	**2.975**

the deviation between the predicted and observed SR in addition to correlation (R) between them. Fig. 5 shows that the proposed ANFIS-muSG model has better prediction capacity over the other comparative models in terms of higher R values during both the modeling phases. There was a noticeable diversion from the ideal line at all the investigated stations. However, the ANFIS-muSG model outputs were noticed least deviated compared to other models.

The box plots were also generated to provide further assessment of the relative performance of the predictive models. Moreover, they also provided more visualized information about the robustness of each model separately. Results obtained during the model testing phase were used for the development of box

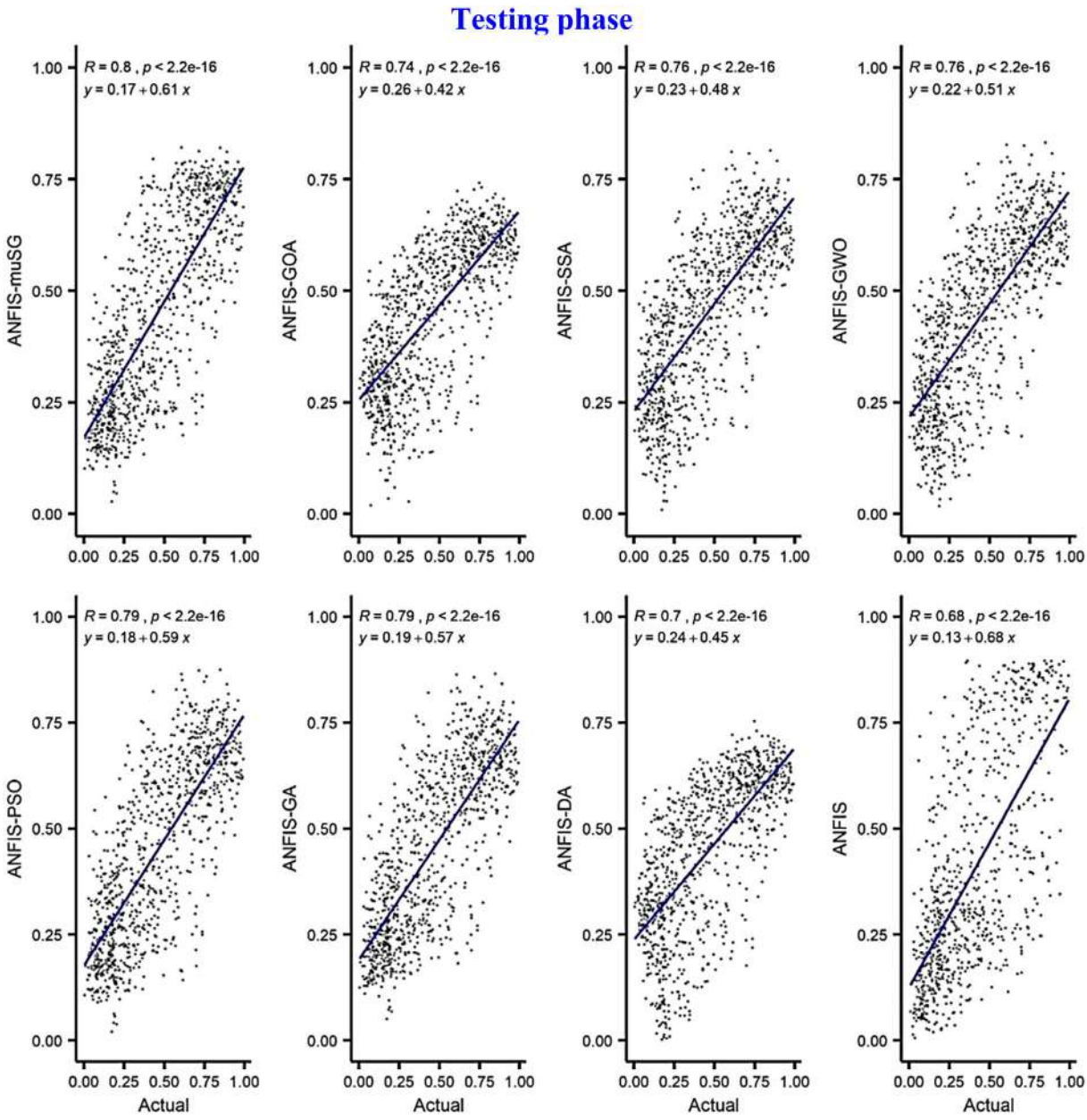

Fig. 5. (*continued*).

Table 6
The statistical performance of solar radiation prediction models during the testing phase at Fingal station (bold represents the best result).

	RMSE MJ/m^2	MAE MJ/m^2	MRE	MARE	RMSRE	AAPRE	R^2	Time
ANFIS-mSG	**0.1715**	**0.1365**	−29.181	**0.516**	**0.976**	**51.516**	**0.769**	49.734
ANFIS-GOA	0.3257	0.2361	−43.621	1.022	4.719	102.121	0.441	65.653
ANFIS-SSA	0.2173	0.1833	−47.581	0.784	2.354	78.368	0.708	11.981
ANFIS-GWO	0.2161	0.1742	**−26.421**	0.695	1.717	69.475	0.697	13.389
ANFIS-PSO	0.1728	0.1372	−29.376	0.518	0.987	51.723	0.765	11.057
ANFIS-GA	0.1728	0.1378	−28.828	0.519	0.990	51.825	0.766	12.309
ANFIS-DA	0.3340	0.2409	−36.174	1.047	6.059	104.552	0.457	19.167
ANFIS	0.3369	0.2815	−73.057	0.965	2.920	96.428	0.694	**5.095**

plots which are presented in Fig. 6. The observed and predicted SR by all the models at Baker station is presented in Fig. 6a. Most of the models were found to predict a few undesirable values or outliers except ANFIS-muSG, ANFIS-PSO, and ANFIS models. Overall, boxes of ANFIS-muSG and ANFIS-PSO were found much similar to the observed one. At Beach station (Fig. 6b), all the models were found to generate outliers except ANFIS. Even though, the median and interquartile range (IQR) of the ANFIS-muSG model were found nearest to the observed median and IQR. Similar results were observed at other locations. The median, IQR, and spread of observed SR data were found to simulate more accurately by ANFIS-muSG model compared to other models.

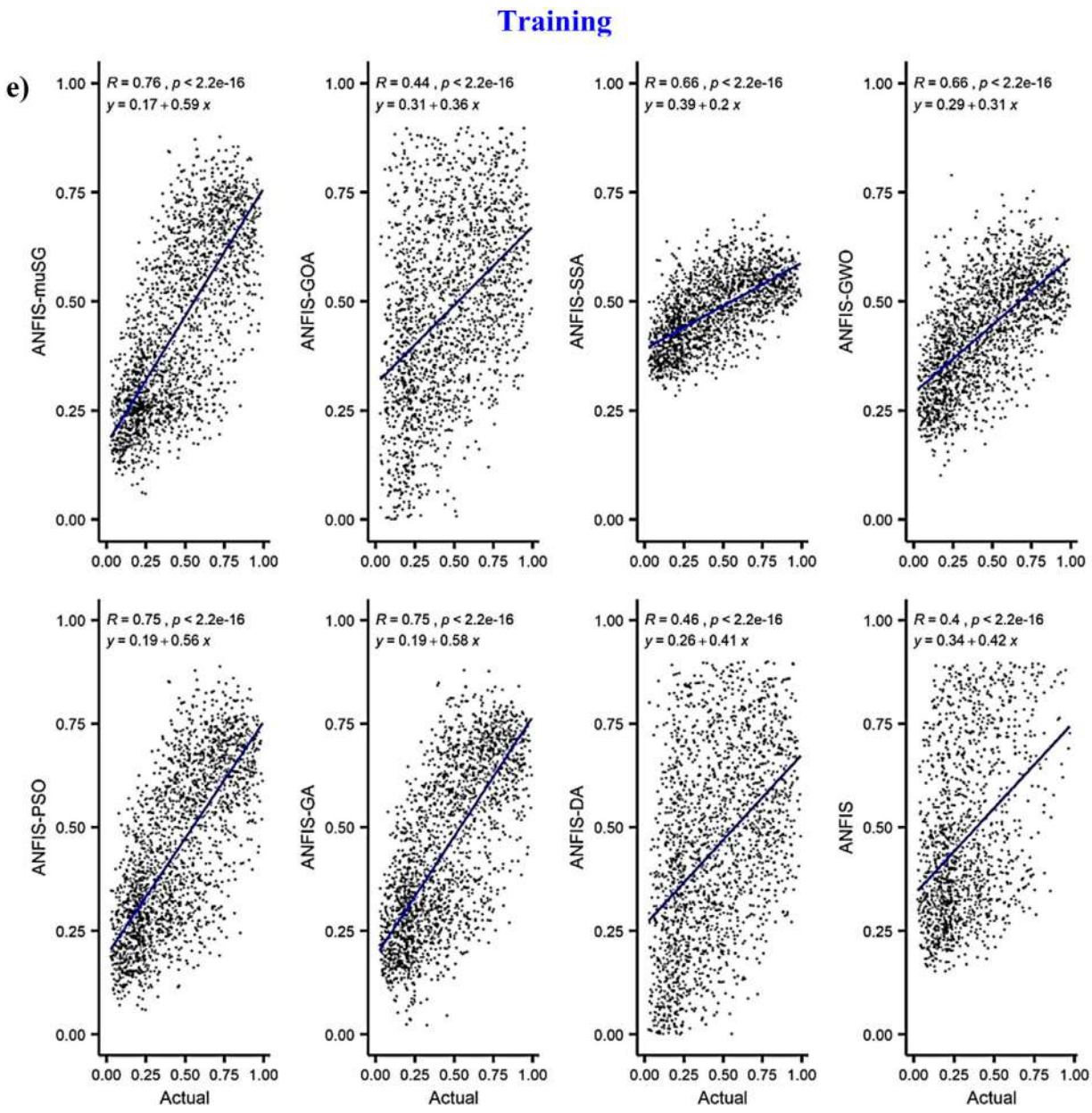

Fig. 5. (*continued*).

The quantitative and visualized information of the performance of all predictive models establishes the superiority of the ANFIS-muSG model over other comparable models in reducing the prediction error. The incorporation of two novel algorithms plays an important role in efficiently optimizing the ANFIS parameters and thereby increasing the accuracy of SR prediction. The adopted predictive model (ANFIS-muSG) in this study exhibited high efficiency in handling intrigue systems such as SR which has several complex characteristics, including, uncertainty, noise, and limited and insufficient information of data.

5. Discussion and possible future research

The results of the study revealed that SR prediction capability can be improved by optimization of ANFIS parameters appropriately. The proposed ANFIS-muSG model reported a significant improvement in terms of performance accuracy compared to classical (ANFIS) and other benchmark hybrid models. The optimization algorithm makes the time of convergence moderately high though in an acceptable range of a few seconds. The study also revealed that better optimization of ANFIS parameters can yield better results. The ANFIS-muSG model was found to perform best due to the employment of an efficient algorithm composed of sophisticated metaheuristic optimization algorithms for the optimization of ANFIS parameters. The results were found consistent at all the locations which confirm the superiority of the ANFIS-muSG approach in different climatic regions of ND.

The models developed in this study may be used for the prediction of SR from temperatures (maximum, mean, and minimum) only which are easily available in any region. Reliable prediction of SR only from temperature parameter indicates the efficacy of the ANFIS-muSG model. Such less resource-demanding models are highly important for developing countries where meteorological data except rainfall and temperature are not easily available. Therefore, the ANFIS-muSG model developed in this study can be employed for energy harvesting and monitoring in a wide range of geographical regions. However, the performance improvement of the model using other meteorological

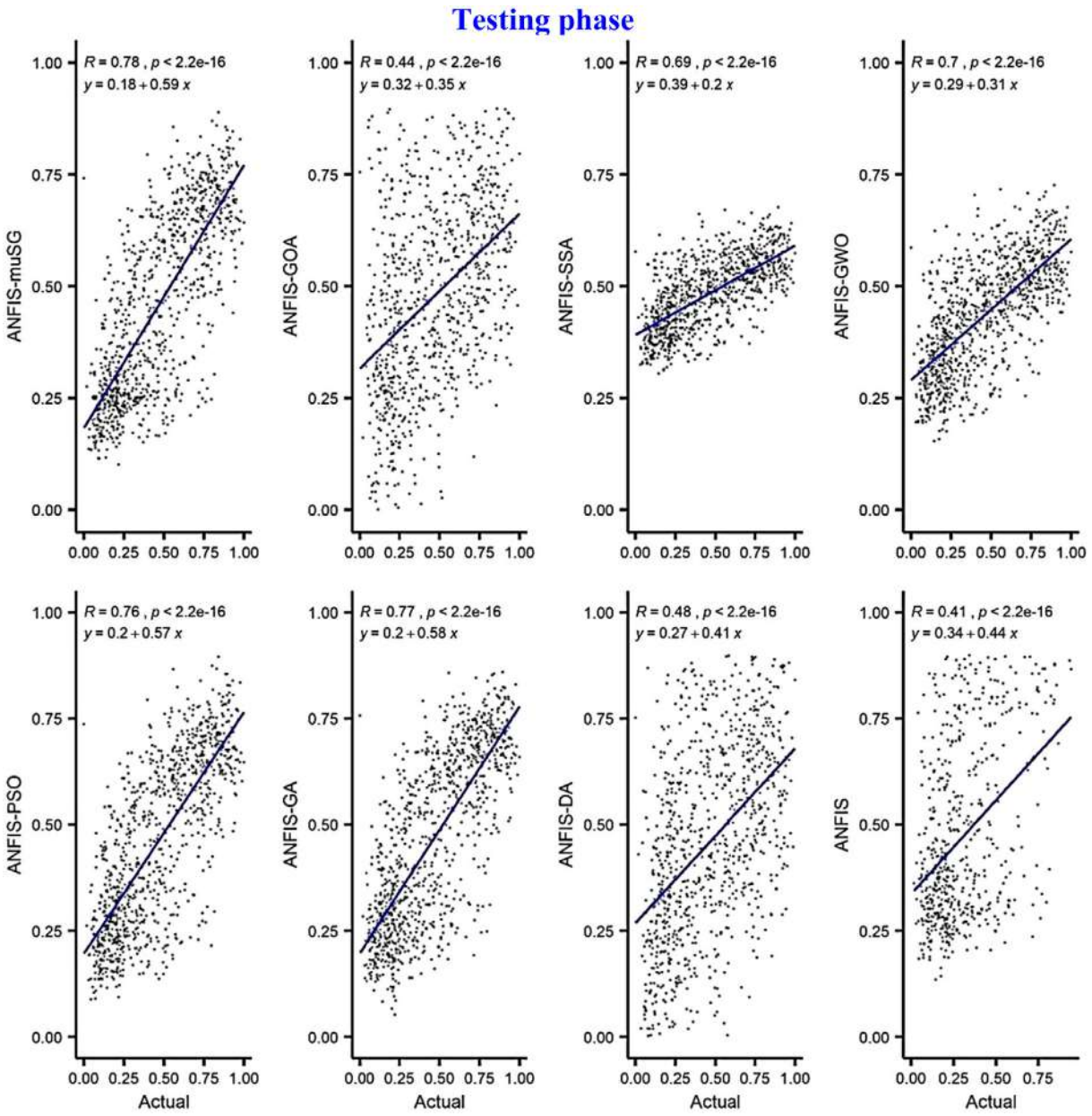

Fig. 5. (*continued*).

variables including wind-speed, cloud cover, sunshine, humidity, and rainfall can be evaluated in future studies. Besides, satellite remote sensing information can be incorporated as input to improve model performance in the prediction of SR (Deo et al., 2019; Ghimire et al., 2019). As process-based models are extensively resource-demanding and cost-prohibitive, the hybrid ANFIS-muSG model developed in this study may be a potential solution.

The performance of the hybridized ANFIS-muSG model could be further improved through an ensemble approach. Besides, other advanced optimization techniques including Quantum-Behaved PSO and the Firefly Algorithm could be utilized to select input predictors that have been found effective in model input selection (Salih et al., 2019; Taormina and Chau, 2015). Besides, empirical wavelet transform (Gilles, 2013) and empirical mode composition (Huang et al., 1998) might be investigated as additional approaches for data analysis.

6. Validation of the proposed model against literature

To provide a fair assessment of the adopted ANFIS-muSG model in the prediction of solar radiation, the findings obtained are compared with previous works carried out in several locations around the world. In this regard, a fair assessment is conducted to validate the accuracy of the adopted model in the prediction of SR. Fan et al. (2018b) employed two AI models for predicting SR over China. The models called SVR and XGBoost were developed based on few metrological factors such as daily maximum and minimum air temperature and rainfall. The outcomes of this study revealed that the SVM provided much more accuracy during model testing than the XGBoost approach. The correlation of determination (R^2) was found as 0.76 and 0.74 for SVM and XGBoost models respectively. Another study conducted by Feng et al. (2019) for the prediction of SR based on only air temperature, where four different AI models were employed like Artificial neural network (ANN), Hybrid mind evolutionary algorithm and artificial neural network (MEA-ANN), Random forests (RF), and

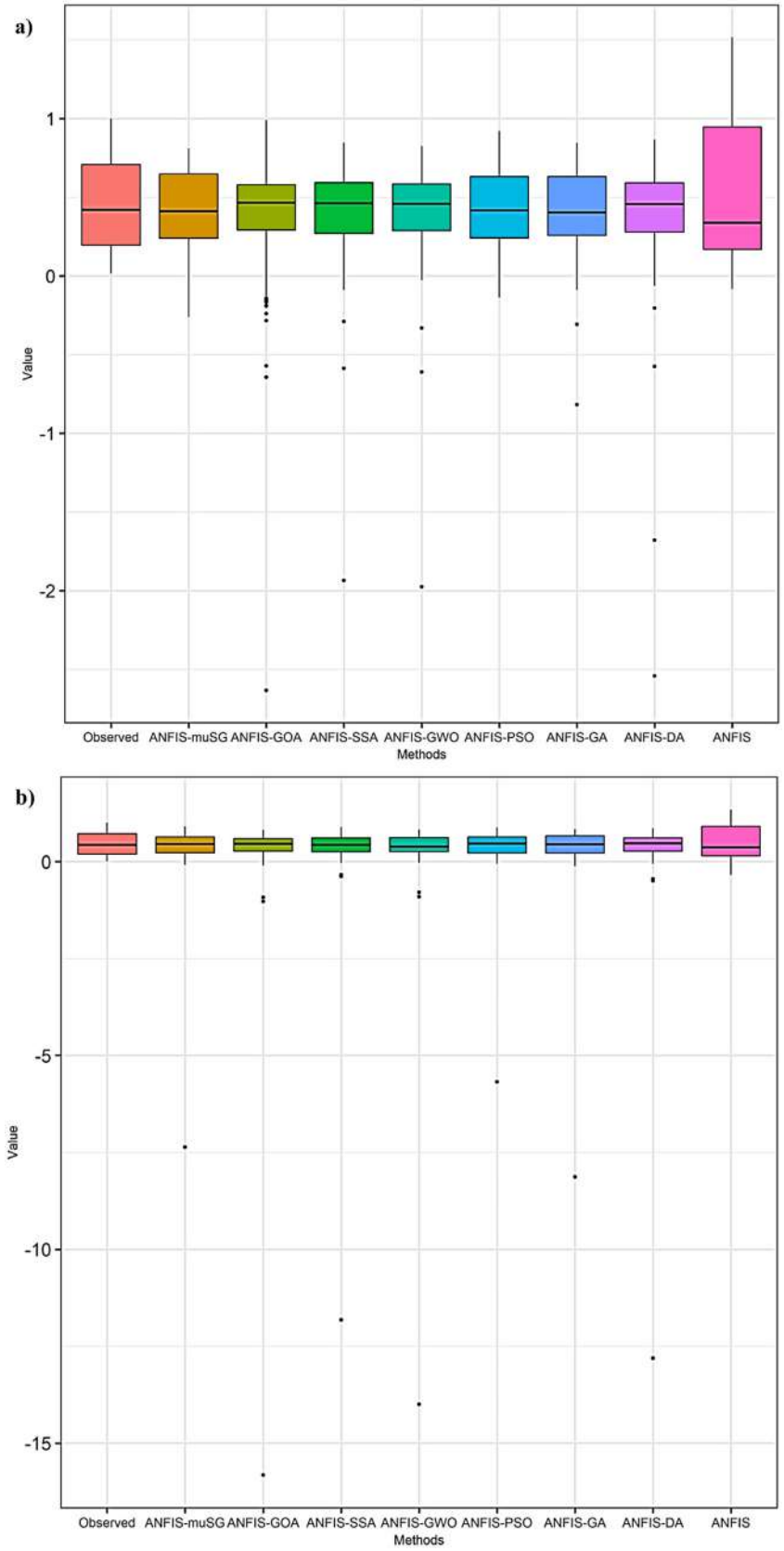

Fig. 6. The box plots of observed and simulated solar radiation by different models at (a) Baker, (b) Beach, (c) Cando, (d) Crary and (e) Fingal station.

Wavelet neural network (WANN). The outcomes of the study showed that MEA-ANN approaches provided the highest accuracy in forecasting the SR ($R^2 = 0.74$). Manju and Sandeep (2019) proposed eight empirical models to estimate the monthly average global SR at twelve locations around India. To achieve a realistic model, they used only sunshine for constructing the predictive

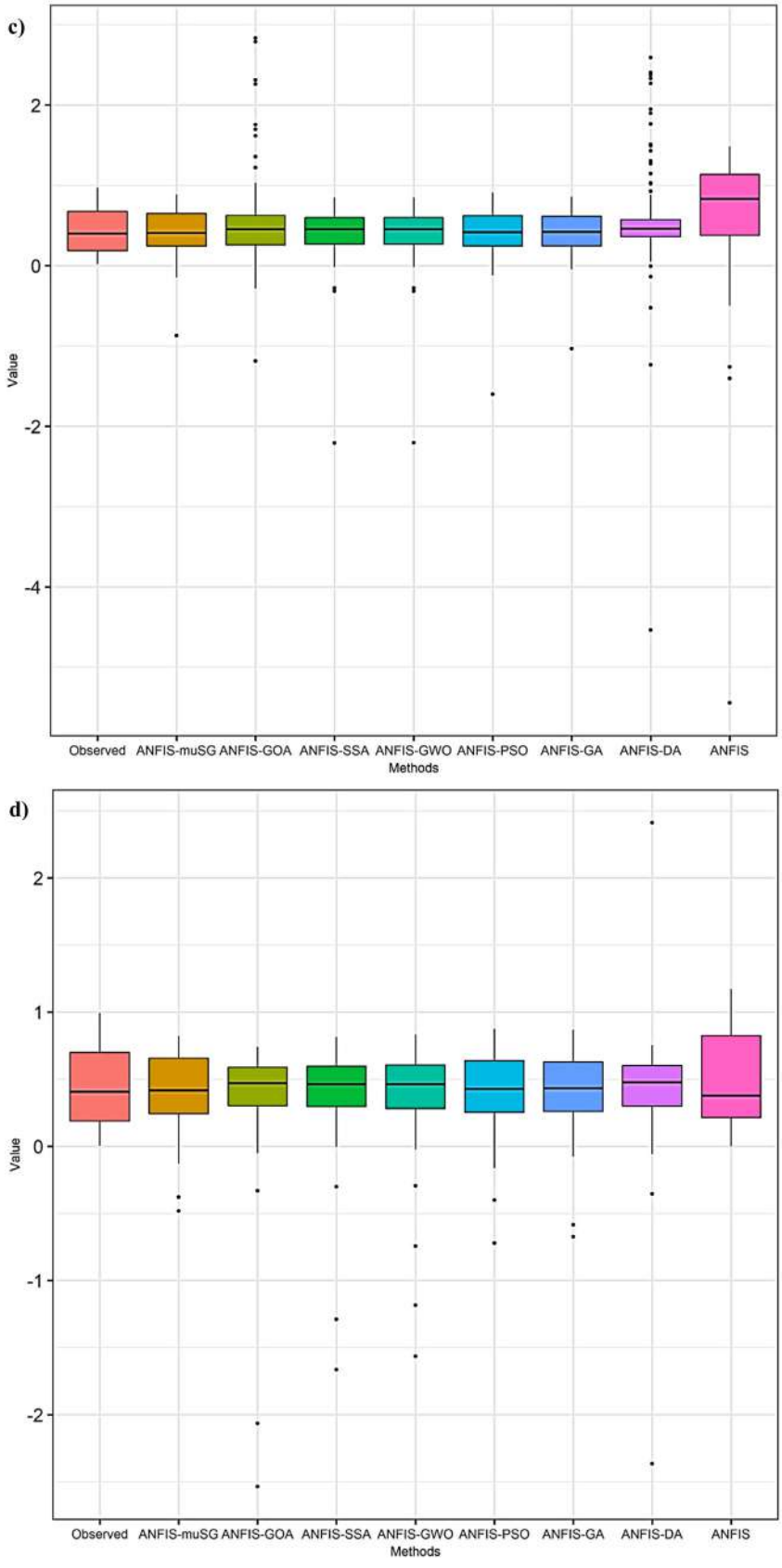

Fig. 6. (*continued*).

models. Based on statistical indices, they concluded that the value of R^2 ranged from 0.6096 to 0.6639 and 0.3416 to 0.4473 respectively for Ahmedabad and Shillong stations. Furthermore, a study conducted by Fan et al. (2020) aimed at prediction of daily diffuse SR in air-polluted regions in China using hybrid SVM approaches such as SVM-PSO, SVM-WOA, SVM-BAT and

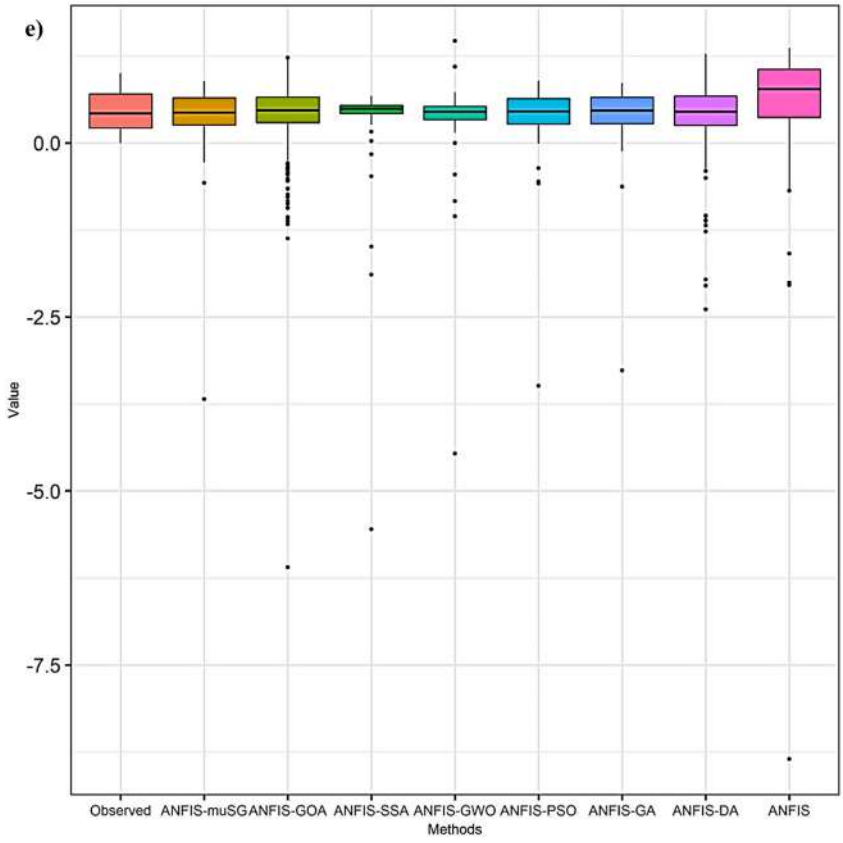

Fig. 6. (*continued*).

other comparable models like extreme gradient boosting (XGBoost), and multivariate adaptive regression spline (MARS). The five models were developed based on several input combinations including, metrological and air pollutes variables. Herein, we only reviewed the models developed based on metrological variables (maximum and minimum temperatures). It can be concluded from the reviewed literature that the models, in general, perform well with the value of R^2 varied from 0.799 to 0.753. Besides, the study by Olatomiwa et al. (2015) carried out to predict global SR over Nigeria using a hybrid SVM-FFA model based on three metrological variables (maximum and minimum temperature and sun duration) showed that the model achieved adequate accuracy with R^2 of 0.728.

It is important to mention that the proposed ANFIS-muSG model of this study achieved a desirable accuracy in comparison with previous studies in the literature. The most interesting observation can be drawn that almost all the previous SR prediction model was developed based on several parameters. However, the model proposed in this study was constructed based on only temperature and it achieved a satisfactory performance with R^2 in the range of 0.769 to 0.802.

7. Conclusion

In this research, the applicability of novel hybridized ANFIS-muSG in predicting daily SR was assessed. The better performance of the proposed ANFIS-muSG model was validated against six hybrid predictive models namely ANFIS-GOA, ANFIS-SSA, ANFIS-GWO, ANFIS-PSO, ANFIS-GA, ANFIS-DA in addition to the standalone ANFIS model. The results indicated a significant improvement in ANFIS model performance through the optimization of its internal parameters. The following research findings are summarized from this study

- Among the hybrid model, the performance of ANFIS-muSG was found best due to better optimization of model parameters.
- In the ANFIS-muSG model, the optimization performance of SSA is improved by using mutation and the improved SSA framework is subsequently used in the GOA algorithm for local searching of optimal values. This helped to improve the performance of ANFIS-muSG compared to other hybrid ANFIS models.
- The ANFIS-muSG showed a prediction enhancement compared to the classical ANFIS model by 42.2%, 32.6, 54.8%, 25.7%, and 49.0% in terms of RMSE at Baker, Beach, Cando, Crary and Fingal stations, respectively.
- Although the proposed algorithm had successfully incorporated with ANFIS approach and reported desirable accuracy in several cases, it provided slightly higher error in some cases. Many reasons may explain this phenomenon, including high noise in the dataset as well as properties of uncertainty and stochastic. Furthermore, the exogenous parameters such as wind speed, cloud cover, sunshine, humidity, and rainfall affect the accuracy of the predictive model. However, the outcomes of the ANFIS-muSG model were very convincing compared to the results obtained in previous studies regarding the prediction of SR.
- It can be concluded that the performance of the hybridized ANFIS-muSG model proved the applicability of the muSG algorithm in optimizing ANFIS parameters when only a single predictor (i.e., air temperature) is used. This indicates the potential of the proposed model for widespread application for accurate prediction of SR.

CRediT authorship contribution statement

Hai Tao: Conceptualization, Writing - original draft, Writing - review & editing. **Ahmed A. Ewees:** Methodology, Software, Writing - original draft, Writing - review & editing. **Ali Omran Al-Sulttani:** Data curation, Writing - original draft, Writing - review & editing. **Ufuk Beyaztas:** Writing - original draft, Writing - review & editing. **Mohammed Majeed Hameed:** Visualization, Writing - original draft, Writing - review & editing. **Sinan Q. Salih:** Data curation, Visualization, Writing - original draft, Writing - review & editing. **Asaad M. Armanuos:** Data curation, Visualization, Writing - original draft, Writing - review & editing. **Nadhir Al-Ansari:** Research funding, Writing - original draft, Writing - review & editing. **Cyril Voyant:** Conceptualization, Writing - original draft, Writing - review & editing. **Shamsuddin Shahid:** Conceptualization, Writing - original draft, Writing - review & editing. **Zaher Mundher Yaseen:** Conceptualization, Project administrative, Writing - original draft, Writing - review & editing.

Declaration of competing interest

The authors declare that they have no known competing financial interests or personal relationships that could have appeared to influence the work reported in this paper.

Acknowledgments

The authors acknowledged their appreciation and gratitude to the North Dakota Agricultural Weather Network (NDAWN), for the dataset used in the current research. Also, the authors reveal their highly appreciation to the respected editors and reviewers for their constructive comments on the presented research. Further, we acknowledge the support received from the Key Research and Development Program in Shaanxi Province (2020GY-078).

References

Abedinia, O., Zareinejad, M., Doranehgard, M.H., Fathi, G., Ghadimi, N., 2019. Optimal offering and bidding strategies of renewable energy based large consumer using a novel hybrid robust-stochastic approach. J. Cleaner Prod. 215, 878–889. http://dx.doi.org/10.1016/j.jclepro.2019.01.085.

Alipour, M., Alighaleh, S., Hafezi, R., Omranievardi, M., 2017. A new hybrid decision framework for prioritizing funding allocation to Iran's energy sector. Energy 121, 388–402.

AlOmar, M.K., Hameed, M.M., AlSaadi, M.A., 2020. Multi hours ahead prediction of surface ozone gas concentration: Robust artificial intelligence approach. Atmos. Pollut. Res. http://dx.doi.org/10.1016/j.apr.2020.06.024.

Awasthi, A., Shukla, A.K., Murali Manohar, S.R., Dondariya, C., Shukla, K.N., Porwal, D., Richhariya, G., 2020. Review on sun tracking technology in solar PV system. Energy Rep. http://dx.doi.org/10.1016/j.egyr.2020.02.004.

Badescu, V., Gueymard, C.A., Cheval, S., Oprea, C., Baciu, M., Dumitrescu, A., Iacobescu, F., Milos, I., Rada, C., 2013. Accuracy analysis for fifty-four clear-sky solar radiation models using routine hourly global irradiance measurements in Romania. Renew. Energy 55, 85–103.

Bagal, H.A., Soltanabad, Y.N., Dadjuo, M., Wakil, K., Ghadimi, N., 2018. Risk-assessment of photovoltaic-wind-battery-grid based large industrial consumer using information gap decision theory. Sol. Energy 169, 343–352. http://dx.doi.org/10.1016/j.solener.2018.05.003.

Ben Othman, A., Belkilani, K., Besbes, M., 2018. Global solar radiation on tilted surfaces in Tunisia: Measurement, estimation and gained energy assessments. Energy Rep. http://dx.doi.org/10.1016/j.egyr.2017.10.003.

Benmouiza, K., Cheknane, A., 2016. Small-scale solar radiation forecasting using ARMA and nonlinear autoregressive neural network models. Theoret. Appl. Climatol. 124, 945–958. http://dx.doi.org/10.1007/s00704-015-1469-z.

Beyaztas, U., Salih, S.Q., Chau, K.-W., Al-Ansari, N., Yaseen, Z.M., 2019. Construction of functional data analysis modeling strategy for global solar radiation prediction: application of cross-station paradigm. Eng. Appl. Comput. Fluid Mech. 13, 1165–1181.

Bokde, N.D., Yaseen, Z.M., Andersen, G.B., 2020. Forecasttb—An R package as a test-bench for time series forecasting—Application of wind speed and solar radiation modeling. Energies 13, 2578.

Budiyanto, M.A., Nasruddin, Lubis, M.H., 2020. Turbidity factor coefficient on the estimation of hourly solar radiation in Depok City, Indonesia. Energy Rep. http://dx.doi.org/10.1016/j.egyr.2019.11.152.

Calif, R., Schmitt, F.G., Huang, Y., Soubdhan, T., 2013. Intermittency study of high frequency global solar radiation sequences under a tropical climate. Sol. Energy 98, 349–365. http://dx.doi.org/10.1016/j.solener.2013.09.018.

Castillo, O., Melin, P., 2012. Optimization of type-2 fuzzy systems based on bio-inspired methods: A concise review. Inform. Sci. http://dx.doi.org/10.1016/j.ins.2012.04.003.

Charabi, Y., Gastli, A., Al-Yahyai, S., 2016. Production of solar radiation bankable datasets from high-resolution solar irradiance derived with dynamical downscaling numerical weather prediction model. Energy Rep. http://dx.doi.org/10.1016/j.egyr.2016.05.001.

Deo, R.C., Şahin, M., Adamowski, J.F., Mi, J., 2019. Universally deployable extreme learning machines integrated with remotely sensed MODIS satellite predictors over Australia to forecast global solar radiation: A new approach. Renew. Sustain. Energy Rev. 104, 235–261.

Deo, R.C., Wen, X., Qi, F., 2016. A wavelet-coupled support vector machine model for forecasting global incident solar radiation using limited meteorological dataset. Appl. Energy http://dx.doi.org/10.1016/j.apenergy.2016.01.130.

Dong, Y., Jiang, H., 2019. Global solar radiation forecasting using square root regularization-based ensemble. Math. Probl. Eng. 2019, 9620945. http://dx.doi.org/10.1155/2019/9620945.

Fan, J., Wang, X., Wu, L., Zhang, F., Bai, H., Lu, X., Xiang, Y., 2018a. New combined models for estimating daily global solar radiation based on sunshine duration in humid regions: A case study in south China. Energy Convers. Manag. 156, 618–625.

Fan, J., Wang, X., Wu, L., Zhou, H., Zhang, F., Yu, X., Lu, X., Xiang, Y., 2018b. Comparison of support vector machine and extreme gradient boosting for predicting daily global solar radiation using temperature and precipitation in humid subtropical climates: A case study in China. Energy Convers. Manage. 164, 102–111. http://dx.doi.org/10.1016/j.enconman.2018.02.087.

Fan, J., Wu, L., Ma, X., Zhou, H., Zhang, F., 2020. Hybrid support vector machines with heuristic algorithms for prediction of daily diffuse solar radiation in air-polluted regions. Renew. Energy 145, 2034–2045.

Fan, J., Wu, L., Zhang, F., Cai, H., Wang, X., Lu, X., Xiang, Y., 2018c. Evaluating the effect of air pollution on global and diffuse solar radiation prediction using support vector machine modeling based on sunshine duration and air temperature. Renew. Sustain. Energy Rev. 94, 732–747.

Feng, Y., Gong, D., Zhang, Q., Jiang, S., Zhao, L., Cui, N., 2019. Evaluation of temperature-based machine learning and empirical models for predicting daily global solar radiation. Energy Convers. Manage. 198, 111780.

Feng, Y., Hao, W., Li, H., Cui, N., Gong, D., Gao, L., 2020. Machine learning models to quantify and map daily global solar radiation and photovoltaic power. Renew. Sustain. Energy Rev. http://dx.doi.org/10.1016/j.rser.2019.109393.

Feng, L., Lin, A., Wang, L., Qin, W., Gong, W., 2018. Evaluation of sunshine-based models for predicting diffuse solar radiation in China. Renew. Sustain. Energy Rev. 94, 168–182. http://dx.doi.org/10.1016/j.rser.2018.06.009.

Gao, W., Darvishan, A., Toghani, M., Mohammadi, M., Abedinia, O., Ghadimi, N., 2019. Different states of multi-block based forecast engine for price and load prediction. Int. J. Electr. Power Energy Syst. 104, 423–435. http://dx.doi.org/10.1016/j.ijepes.2018.07.014.

Ghadimi, N., Akbarimajd, A., Shayeghi, H., Abedinia, O., 2018. Two stage forecast engine with feature selection technique and improved meta-heuristic algorithm for electricity load forecasting. Energy 161, 130–142. http://dx.doi.org/10.1016/j.energy.2018.07.088.

Ghimire, S., Deo, R.C., Raj, N., Mi, J., 2019. Wavelet-based 3-phase hybrid SVR model trained with satellite-derived predictors, particle swarm optimization and maximum overlap discrete wavelet transform for solar radiation prediction. Renew. Sustain. Energy Rev. 113, 109247.

Gilles, J., 2013. Empirical wavelet transform. IEEE Trans. Signal Process. 61, 3999–4010. http://dx.doi.org/10.1109/tsp.2013.2265222.

Gouda, S.G., Hussein, Z., Luo, S., Wang, P., Cao, H., Yuan, Q., 2018. Empirical models for estimating global solar radiation in Wuhan City, China. Eur. Phys. J. Plus 133 (517).

Hafezi, R., Bahrami, M., Akhavan, A.N., 2017. Sustainability in development: rethinking about old paradigms. World Rev. Sci. Technol. Sustain. Dev. 13, 192–204.

Hai, T., Sharafati, A., Mohammed, A., Salih, S.Q., Deo, R.C., Al-Ansari, N., Yaseen, Z.M., 2020. Global solar radiation estimation and climatic variability analysis using extreme learning machine based predictive model. IEEE Access 8, 12026–12042. http://dx.doi.org/10.1109/ACCESS.2020.2965303.

Halabi, L.M., Mekhilef, S., Hossain, M., 2018. Performance evaluation of hybrid adaptive neuro-fuzzy inference system models for predicting monthly global solar radiation. Appl. Energy 213, 247–261. http://dx.doi.org/10.1016/j.apenergy.2018.01.035.

Hassan, G.E., Youssef, M.E., Mohamed, Z.E., Ali, M.A., Hanafy, A.A., 2016. New temperature-based models for predicting global solar radiation. Appl. Energy 179, 437–450. http://dx.doi.org/10.1016/j.apenergy.2016.07.006.

Hou, M., Zhang, T., Weng, F., Ali, M., Al-Ansari, N., Yaseen, Z., 2018. Global solar radiation prediction using hybrid online sequential extreme learning machine model. Energies 11 (3415).

Huang, N.E., Shen, Z., Long, S.R., Wu, M.C., Snin, H.H., Zheng, Q., Yen, N.C., Tung, C.C., Liu, H.H., 1998. The empirical mode decomposition and the hubert spectrum for nonlinear and non-stationary time series analysis. Proc. R. Soc. A Math. Phys. Eng. Sci. http://dx.doi.org/10.1098/rspa.1998.0193.

Hussain, S., Alili, 2017. A pruning approach to optimize synaptic connections and select relevant input parameters for neural network modelling of solar radiation. Appl. Soft Comput. 52, 898–908. http://dx.doi.org/10.1016/j.asoc.2016.09.036.

Jang, J.S.R., Sun, C.T., 1995. Neuro-fuzzy modeling and control. Proc. IEEE http://dx.doi.org/10.1109/5.364486.

Jiang, H., Dong, Y., Wang, J., Li, Y., 2015. Intelligent optimization models based on hard-ridge penalty and RBF for forecasting global solar radiation. Energy Convers. Manage. 95, 42–58. http://dx.doi.org/10.1016/j.enconman.2015.02.020.

Katebi, J., Shoaei-parchin, M., Shariati, M., Trung, N.T., Khorami, M., 2019. Developed comparative analysis of metaheuristic optimization algorithms for optimal active control of structures. Eng. Comput. 1–20.

Kisi, O., Heddam, S., Yaseen, Z.M., 2019. The implementation of univariable scheme-based air temperature for solar radiation prediction: New development of dynamic evolving neural-fuzzy inference system model. Appl. Energy 241, 184–195.

Kisi, O., Yaseen, Z.M., 2019. The potential of hybrid evolutionary fuzzy intelligence model for suspended sediment concentration prediction. CATENA 174, 11–23.

Loghmari, I., Timoumi, Y., Messadi, A., 2018. Performance comparison of two global solar radiation models for spatial interpolation purposes. Renew. Sustain. Energy Rev. 82, 837–844. http://dx.doi.org/10.1016/j.rser.2017.09.092.

Manju, S., Sandeep, M., 2019. Prediction and performance assessment of global solar radiation in Indian cities: A comparison of satellite and surface measured data. J. Cleaner Prod. 230, 116–128. http://dx.doi.org/10.1016/j.jclepro.2019.05.108.

Mathew, A., Sreekumar, S., Khandelwal, S., Kumar, R., 2019. Prediction of land surface temperatures for surface urban heat island assessment over Chandigarh city using support vector regression model. Sol. Energy 186, 404–415. http://dx.doi.org/10.1016/j.solener.2019.04.001.

Mirjalili, S., Gandomi, A.H., Mirjalili, S.Z., Saremi, S., Faris, H., Mirjalili, S.M., 2017. Salp swarm algorithm: A bio-inspired optimizer for engineering design problems. Adv. Eng. Softw. 1–29. http://dx.doi.org/10.1016/j.advengsoft.2017.07.002.

Mohammadi, K., Shamshirband, S., Kamsin, A., Lai, P.C., Mansor, Z., 2016. Identifying the most significant input parameters for predicting global solar radiation using an ANFIS selection procedure. Renew. Sustain. Energy Rev. 63, 423–434. http://dx.doi.org/10.1016/j.rser.2016.05.065.

Mohanty, S., Patra, P.K., Sahoo, S.S., 2016. Prediction and application of solar radiation with soft computing over traditional and conventional approach - a comprehensive review. Renew. Sustain. Energy Rev. 56, 778–796. http://dx.doi.org/10.1016/j.rser.2015.11.078.

Naubi, I., Zardari, N.H., Shirazi, S.M., Ibrahim, N.F.B., Baloo, L., 2016. Effectiveness of water quality index for monitoring Malaysian river water quality. Polish J. Environ. Stud. 25.

Nourani, V., Elkiran, G., Abdullahi, J., Tahsin, A., 2019. Multi-region modeling of daily global solar radiation with artificial intelligence ensemble. Nat. Resour. Res. 1–22.

Okundamiya, M.S., Emagbetere, J.O., Ogujor, E.A., 2016. Evaluation of various global solar radiation models for Nigeria. Int. J. Green Energy 13, 505–512. http://dx.doi.org/10.1080/15435075.2014.968921.

Olatomiwa, L., Mekhilef, S., Shamshirband, S., Mohammadi, K., Petković, D., Sudheer, C., 2015. A support vector machine-firefly algorithm-based model for global solar radiation prediction. Sol. Energy 115, 632–644. http://dx.doi.org/10.1016/j.solener.2015.03.015.

Peel, M.C., Finlayson, B.L., McMahon, T.A., 2007. Updated world map of the Köppen-Geiger climate classification. Hydrol. Earth Syst. Sci. Discuss. 4, 439–473.

Premalatha, M., Naveen, C., 2018. Analysis of different combinations of meteorological parameters in predicting the horizontal global solar radiation with ANN approach: A case study. Renew. Sustain. Energy Rev. 91, 248–258.

Sadeghipour Chahnasir, E., Zandi, Y., Shariati, M., Dehghani, E., Toghroli, A., Tonnizam Mohamad, E., Shariati, A., Safa, M., Wakil, K., Khorami, M., 2018. Application of support vector machine with firefly algorithm for investigation of the factors affecting the shear strength of angle shear connectors. Smart Struct. Syst. http://dx.doi.org/10.12989/sss.2018.22.4.413.

Salih, S.Q., Alsewari, A.A., Al-Khateeb, B., Zolkipli, M.F., 2019. Novel multi-swarm approach for balancing exploration and exploitation in particle swarm optimization. In: Saeed, F., Gazem, N., Mohammed, F., Busalim, A. (Eds.), Recent Trends in Data Science and Soft Computing. Springer International Publishing, Cham, pp. 196–206.

Saremi, S., Mirjalili, S., Lewis, A., 2017. Grasshopper optimisation algorithm: Theory and application. Adv. Eng. Softw. 105, 30–47. http://dx.doi.org/10.1016/j.advengsoft.2017.01.004.

Sedghi, Y., Zandi, Y., Shariati, M., Ahmadi, E., Azar, V.M., Toghroli, A., Safa, M., Mohamad, E.T., Khorami, M., Wakil, K., 2018. Application of ANFIS technique on performance of C and L shaped angle shear connectors. Smart Struct. Syst. http://dx.doi.org/10.12989/sss.2018.22.3.335.

Sharafati, A., Khosravi, K., Khosravinia, P., Ahmed, K., Salman, S.A., Mundher, Z., Shamsuddin, Y., 2019. The potential of novel data mining models for global solar radiation prediction. Int. J. Environ. Sci. Technol. http://dx.doi.org/10.1007/s13762-019-02344-0.

Sutherland, J.C., 2017. Linear dichroism of DNA: Characterization of the orientation distribution function caused by hydrodynamic shear. Anal. Biochem. http://dx.doi.org/10.1016/j.ab.2017.01.016.

Tao, H., Ebtehaj, I., Bonakdari, H., Heddam, S., Voyant, C., Al-ansari, N., Deo, R., Yaseen, Z.M., 2019. Designing a new data intelligence model for global solar radiation prediction : Application of multivariate modeling scheme. pp. 1–24, http://dx.doi.org/10.3390/en12071365.

Taormina, R., Chau, K.W., 2015. Data-driven input variable selection for rainfall-runoff modeling using binary-coded particle swarm optimization and extreme learning machines. J. Hydrol. 529, 1617–1632. http://dx.doi.org/10.1016/j.jhydrol.2015.08.022.

Voyant, C., Notton, G., Duchaud, J.L., Almorox, J., Yaseen, Z.M., 2020. Solar irradiation prediction intervals based on Box–Cox transformation and univariate representation of periodic autoregressive model. Renew. Energy Focus http://dx.doi.org/10.1016/j.ref.2020.04.001.

Voyant, C., Notton, G., Kalogirou, S., Nivet, M.L., Paoli, C., Motte, F., Fouilloy, A., 2017. Machine learning methods for solar radiation forecasting: A review. Renew. Energy 105, 569–582. http://dx.doi.org/10.1016/j.renene.2016.12.095.

Xie, T., Li, J., Sun, C., Ding, R., Wang, K., Zhao, C., Feng, J., 2019. NAO Implicated as a predictor of the surface air temperature multidecadal variability over East Asia. Clim. Dynam. 53, 895–905. http://dx.doi.org/10.1007/s00382-019-04624-4.

Yaseen, Zaher Mundher, Mohtar, Wan Hanna Melini Wan, Ameen Ameen, Mohammed Salih, Ebtehaj, Isa, Razali, Siti Fatin Mohd, Bonakdari, Hossein, Salih, Sinan Q, Al-Ansari, Nadhir, Shahid, Shamsuddihao, 2019. Implementation of univariate paradigm for streamflow simulation using hybrid data-driven model: case study in tropical region. IEEE Access 7, 74471–74481.

Zeng, Z., Yang, H., Zhao, R., Meng, J., 2013. Nonlinear characteristics of observed solar radiation data. Sol. Energy 87, 204–218. http://dx.doi.org/10.1016/j.solener.2012.10.019.

Zhang, G., Ali, Z.H., Aldlemy, M.S., Mussa, M.H., Salih, S.Q., Hameed, M.M., Al-Khafaji, Z.S., Yaseen, Z.M., 2020. Reinforced concrete deep beam shear strength capacity modelling using an integrative bio-inspired algorithm with an artificial intelligence model. Eng. Comput. http://dx.doi.org/10.1007/s00366-020-01137-1.

Zou, L., Wang, L., Lin, A., Zhu, H., Peng, Y., Zhao, Z., 2016. Estimation of global solar radiation using an artificial neural network based on an interpolation technique in southeast China. J. Atmos. Sol.-Terr. Phys. 146, 110–122. http://dx.doi.org/10.1016/j.jastp.2016.05.013.